united nations educational, scientific and cultural organization

international atomic energy agency

the
abdus salam
international centre for theoretical physics

School on "Exploring the Atmosphere by Remote Sensing Techniques"
18 October - 5 November 1999

1151-20

"Aerosol Lidar"

B. Stein
Alfred-Wegener Institut for Polar & Maritime Research
Potsdam
Germany

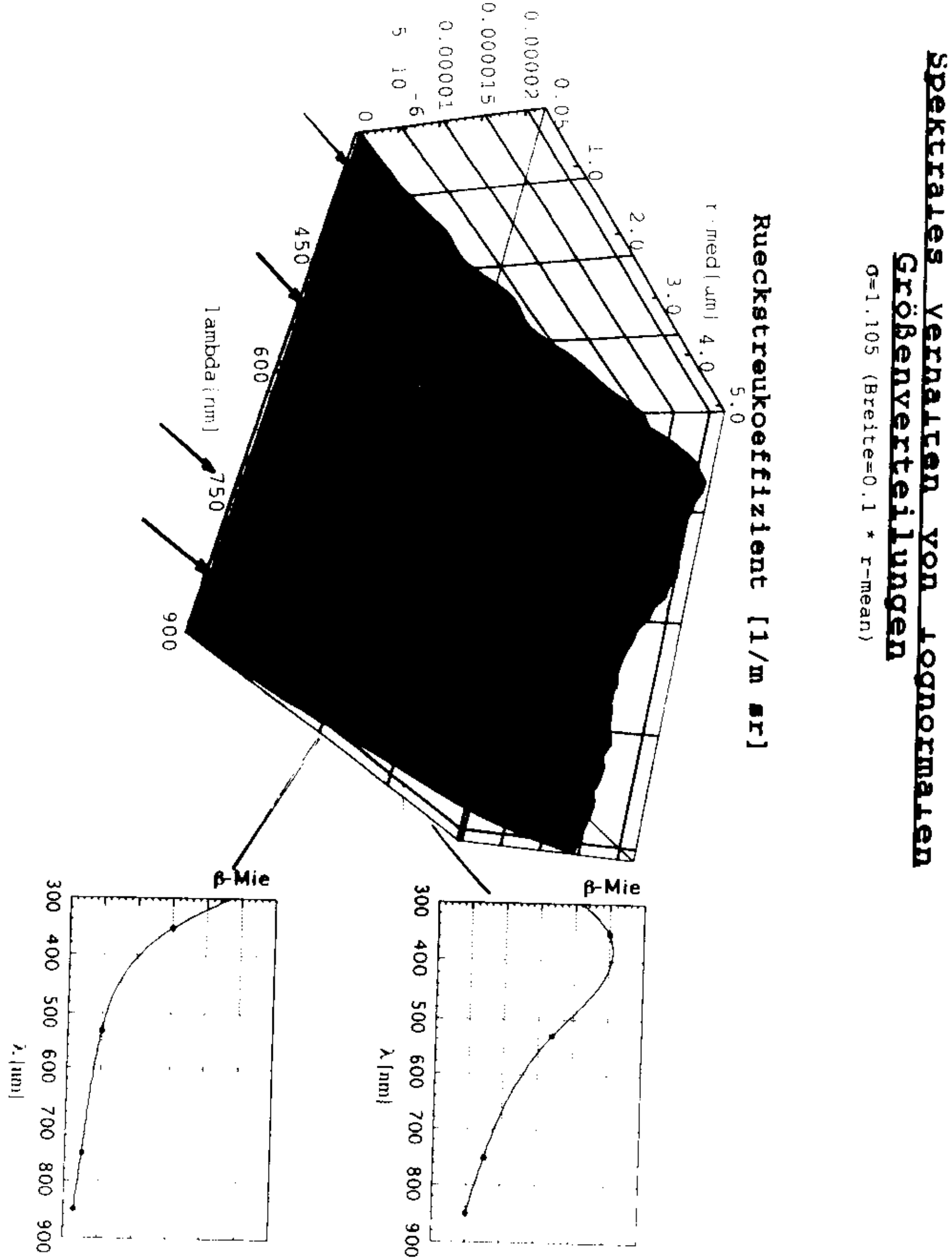

Bernhard Stein
Alfred Wegener Inst. for Polar and Maritime Research
Potsdam, Germany
bstein@awi-potsdam.de

Aerosol Lidar

1. Retrieval of aerosol size distributions (ASD) from multiwavelength lidar measurements:
   - spectral signature, volcanic aerosol, PSCs

2. The Raman lidar technique:

2.1 Aerosol
- what is extinction +how can we measure $\alpha(\lambda)$
- Raman scattering characteristics
- lidar equation for Raman scattering
- experimental setup
- measurement examples

2.2 Trace gas measurements
- Multicomponent analysis
- H_2O measurements

2.3 Temperature measurements
- Rayleigh scattering method
- Rotational Raman scattering method

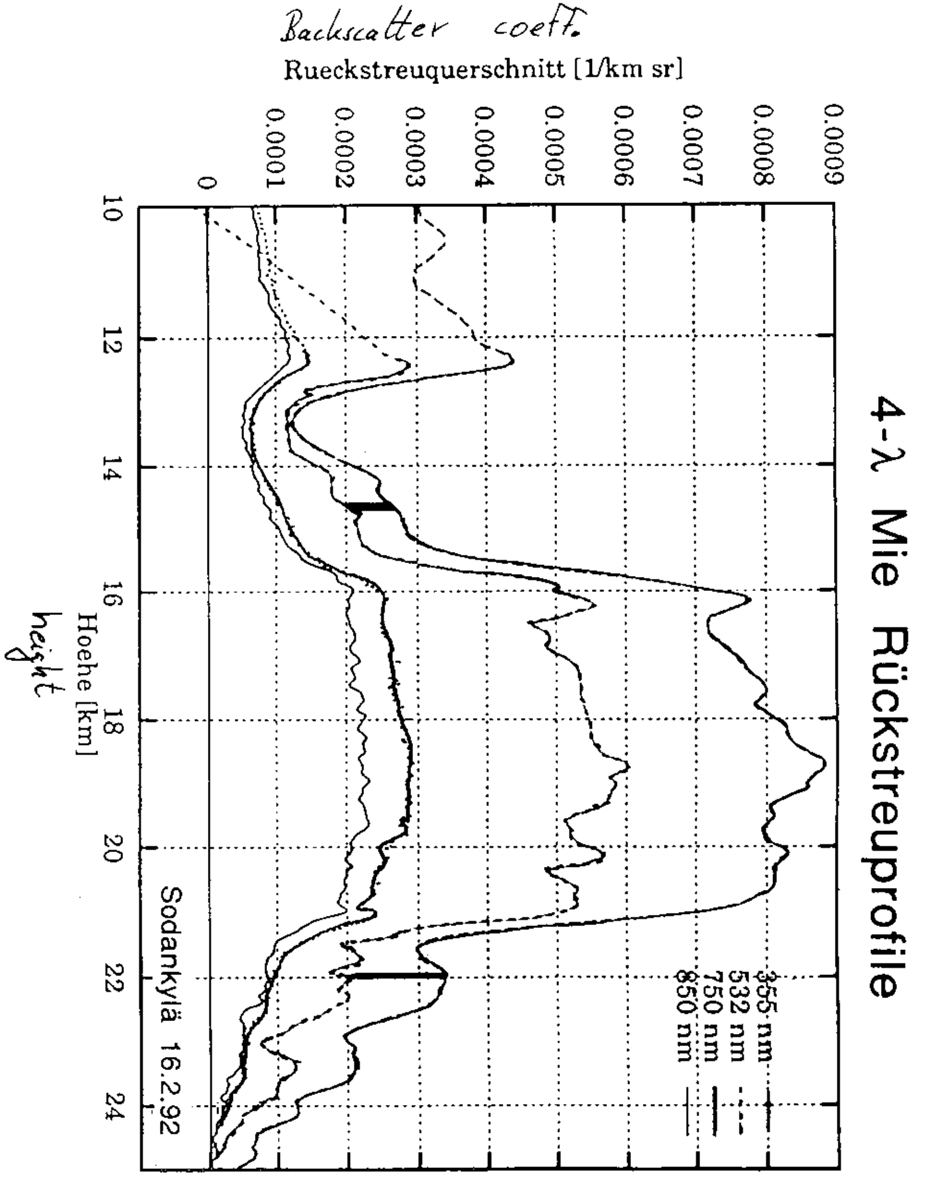

Fit-Parameter χ^2

measured at λ_j — β of size distribution $\rho_s(r,\sigma)$

$$\chi^2 = \sum_{j=1}^{4} \left(\frac{\beta_j - \beta_{sj}\left[\rho_s(r,\sigma)\right]}{\Delta\beta_j} \right)$$

uncertainty at λ_j

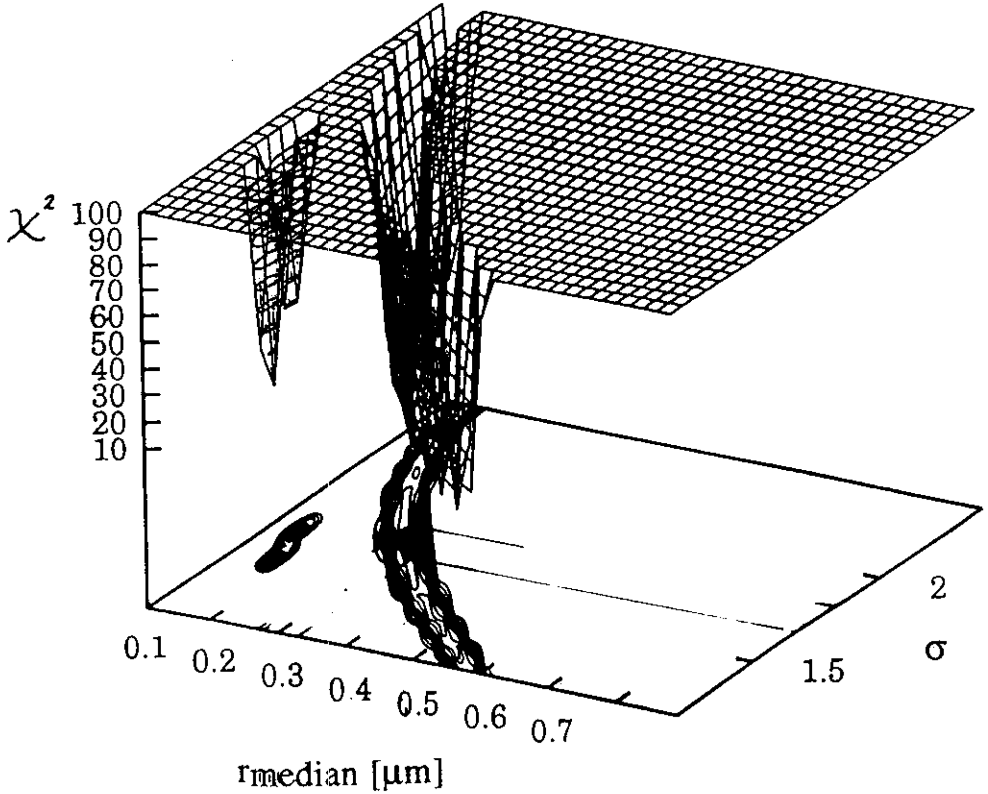

Variation der Fit-Resultate

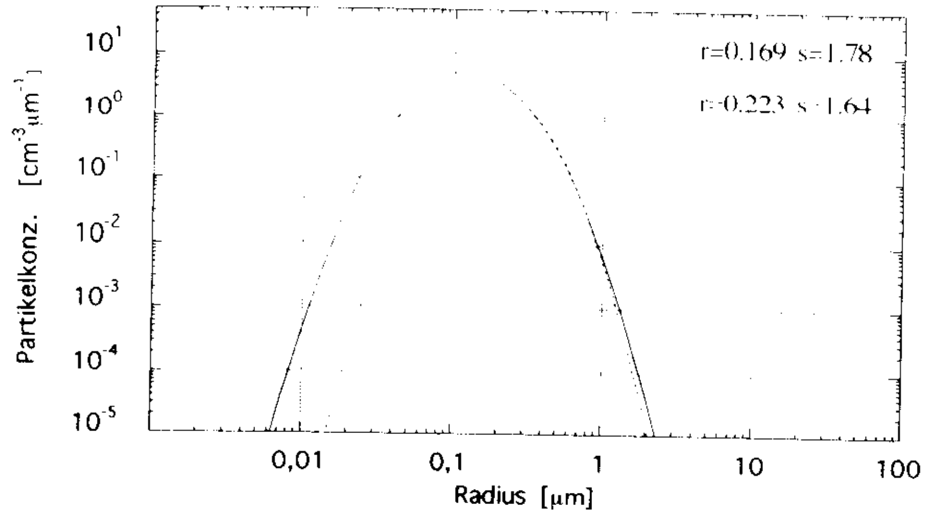

Bimodale Größenverteilung

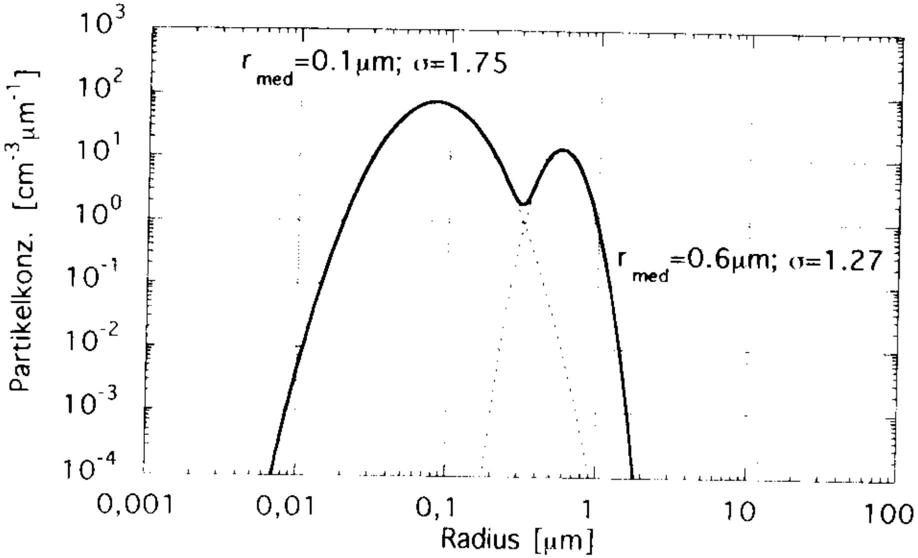

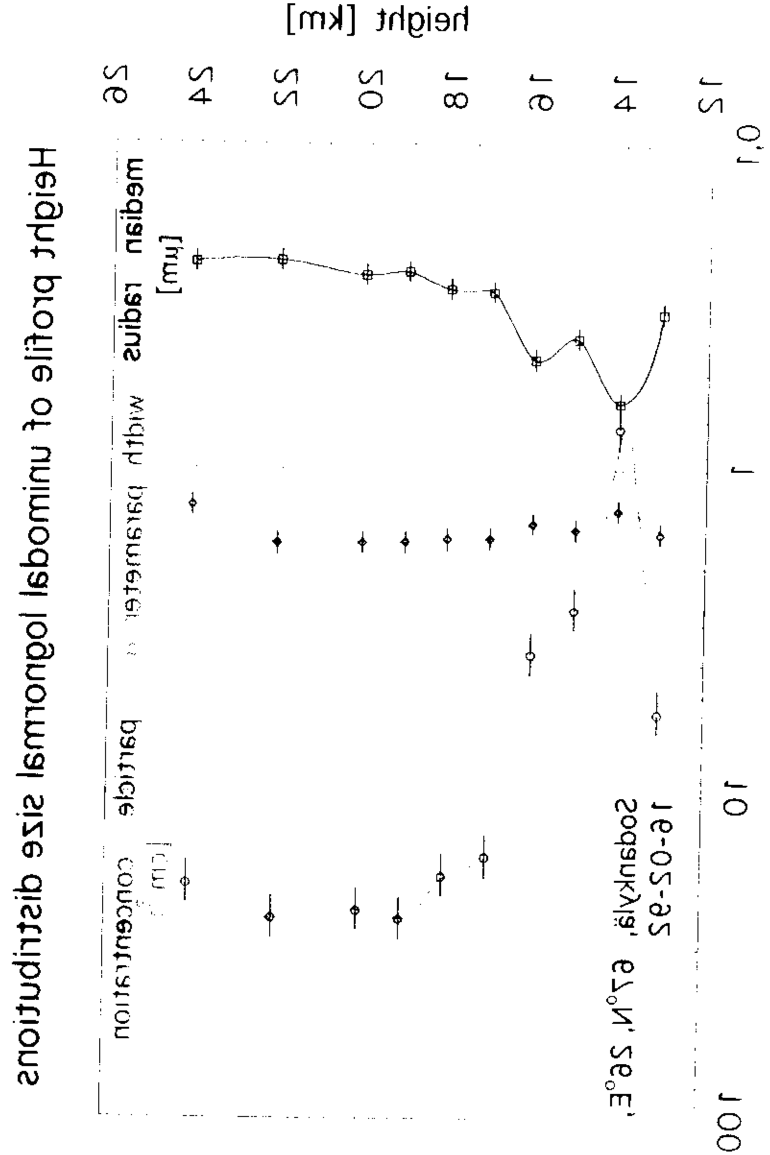

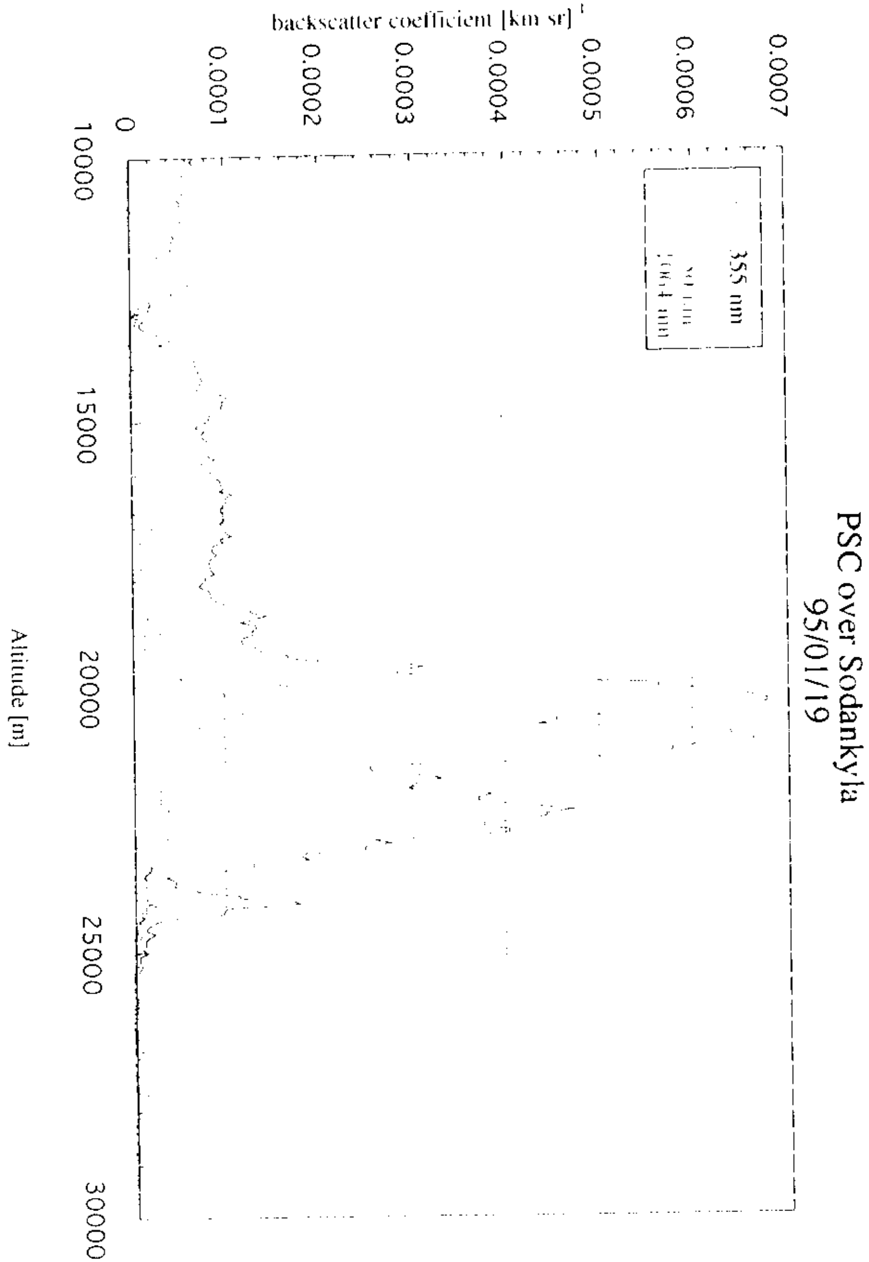

Bimodal AerosolSize Distributions

Comparison of Lidar and balloon measurements

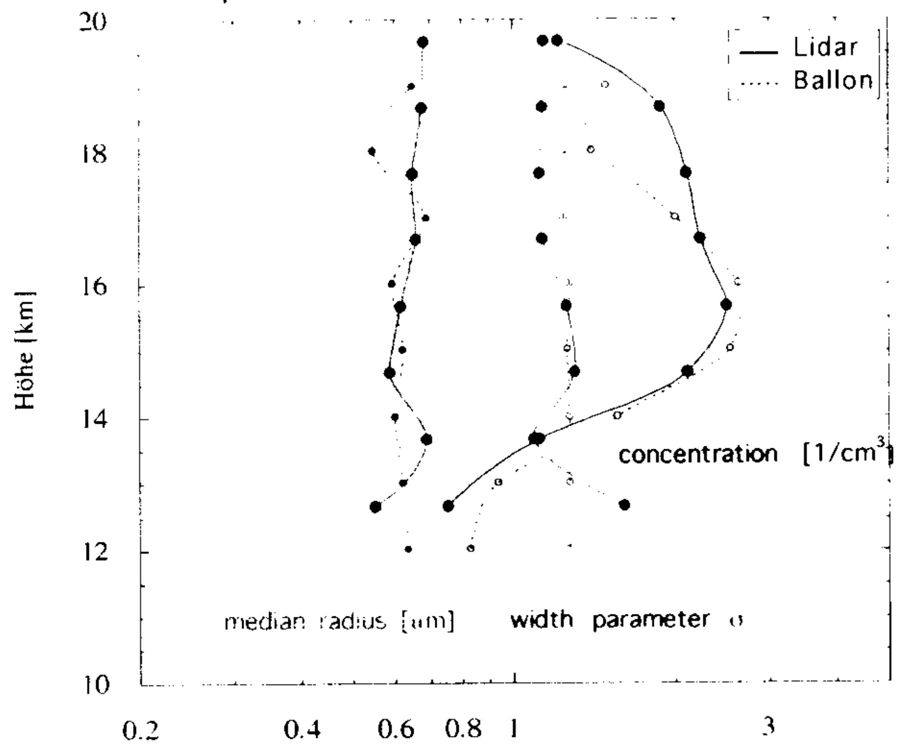

Size distribution of liquid PSC

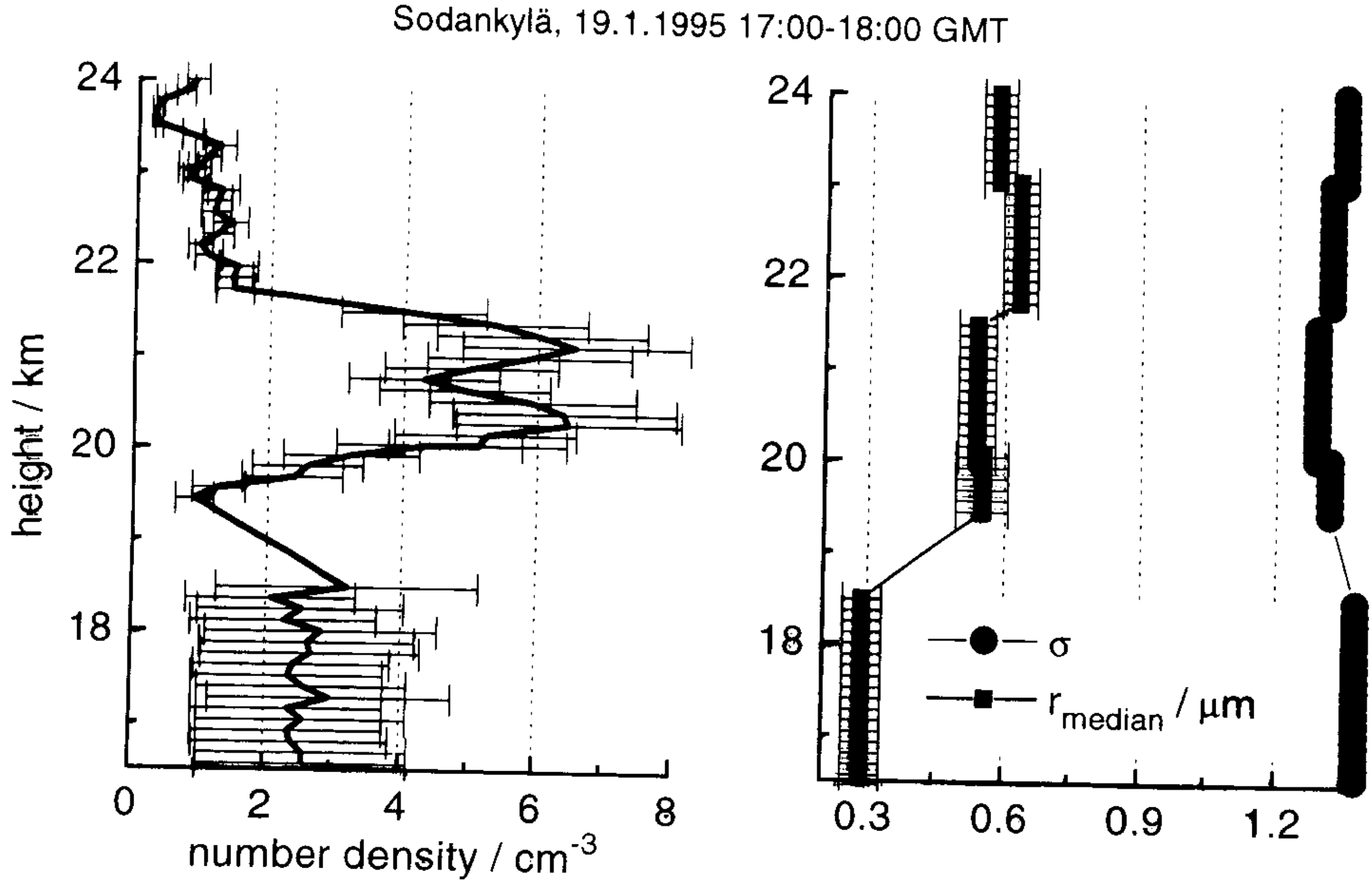

Refractive index of liquid PSC

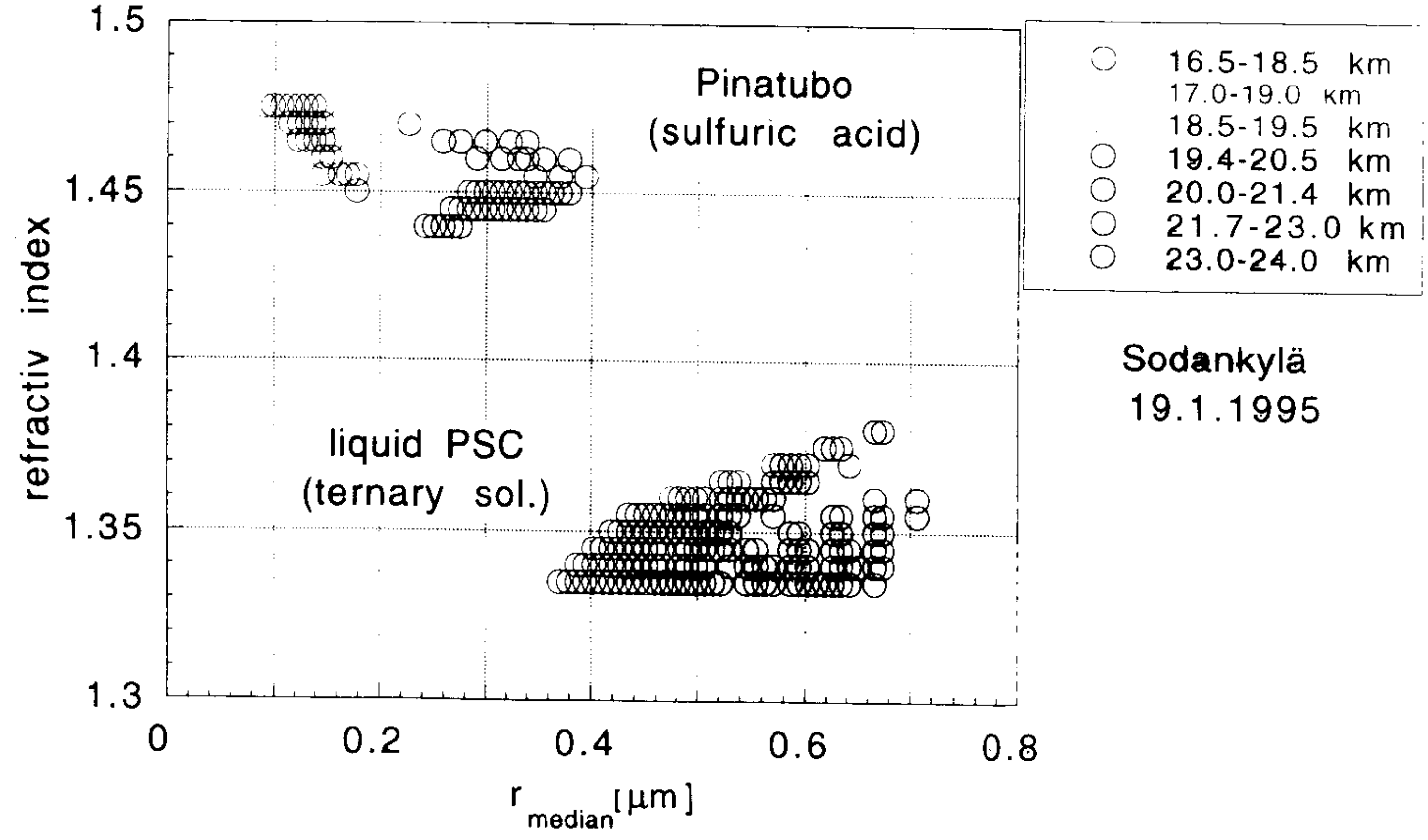

Extinction $\alpha(\lambda)$= **absorption + scattering (360°)**

<u>Why is height resolved aerosol extinction an important parameter?</u>

- aerosol radiative forcing is the major uncertainty to predict longterm temperature trends
- the height (and temperature) of an aerosol layer influences the climate effect
- the „lidar ratio" $\alpha(\lambda)/\beta(\lambda)$ contains information about the aerosol composition and size distribution

<u>A conclusion about aerosol size distribution retrieval by multispectral lidar:</u>

is possible to retrieve ASD parameters (size, refr. index) when

- particles are spherical
- an assumption about the shape of the ASD can be justified
- backscatter coefficients at 3 (better 4) wavelengths can be measured (error<10%)
- no relevant absorption occurs (transparent particles)

Mie-scattering at spherical particles

with different size parameter $ka = \frac{2\pi r}{\lambda}$

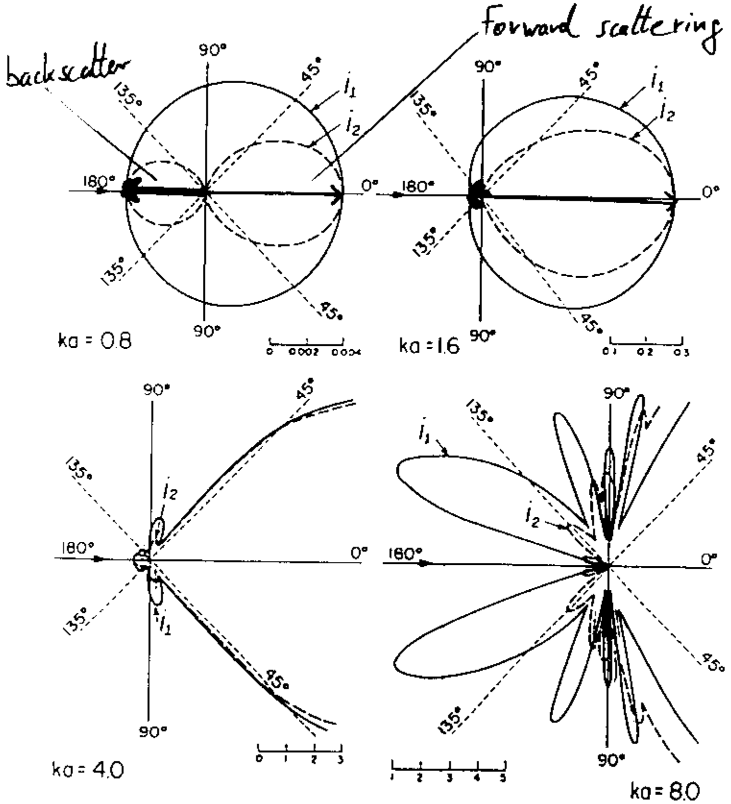

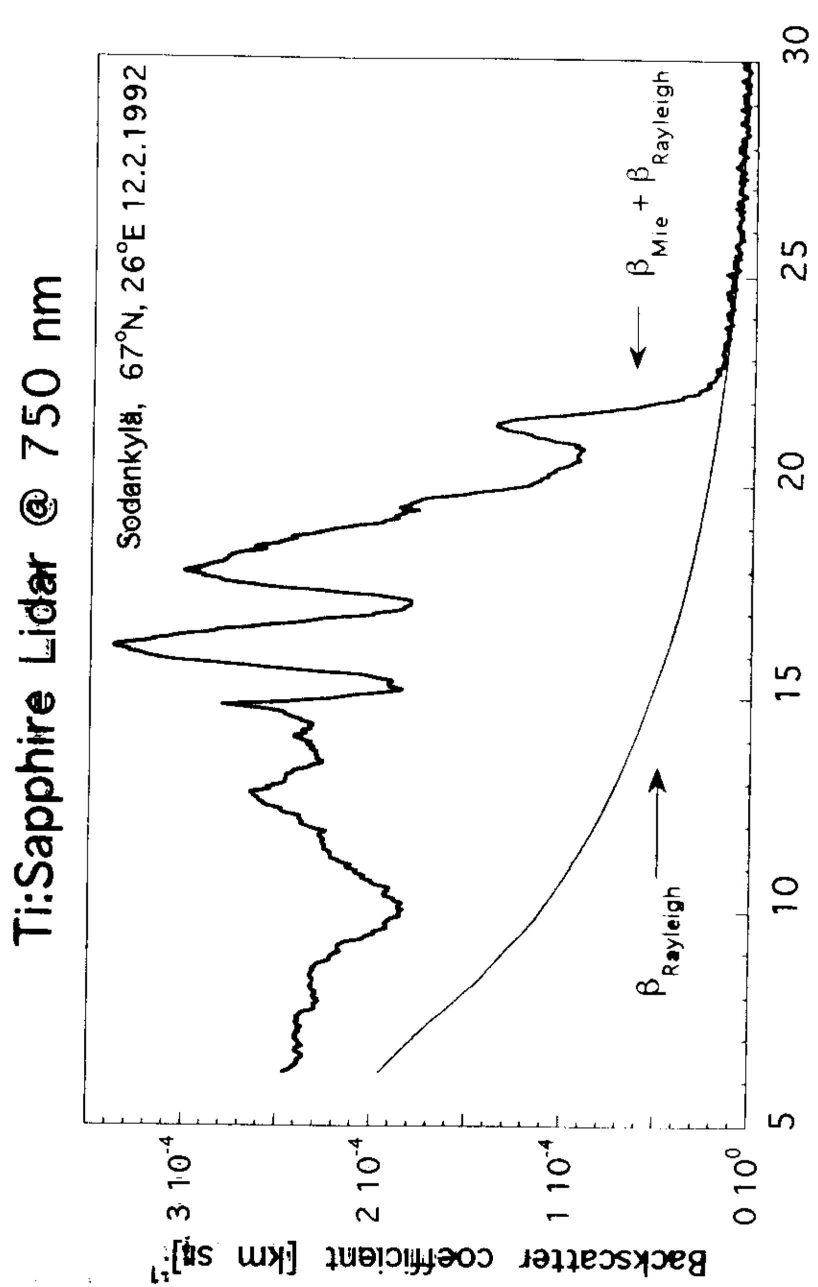

Scattering Processes

Rayleigh scattering
all molecules
$\lambda_{in} = \lambda_{out}$

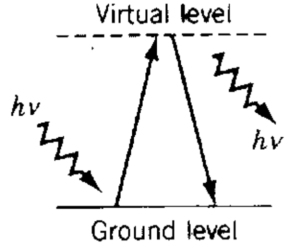

Mie scattering
all spherical particles
$\lambda_{in} = \lambda_{out}$

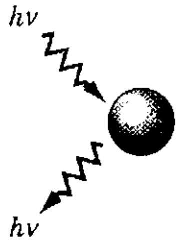

Raman scattering
molecules
$\lambda_{in} \neq \lambda_{out}$

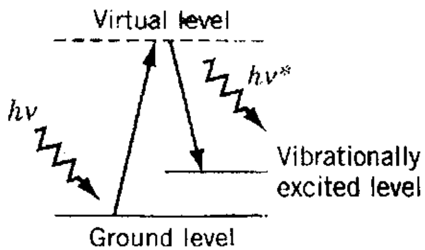

σ=1.105 (Breite=0.1 * r-mean)

Extinktions/Rueckstreukoeffizient [sr]

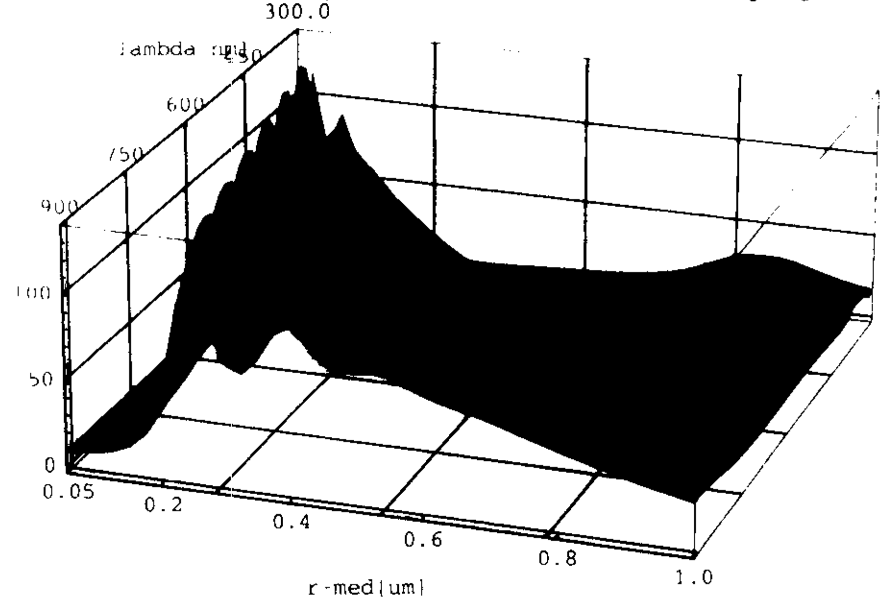

Extinktions/Rueckstreukoeffizient [sr]

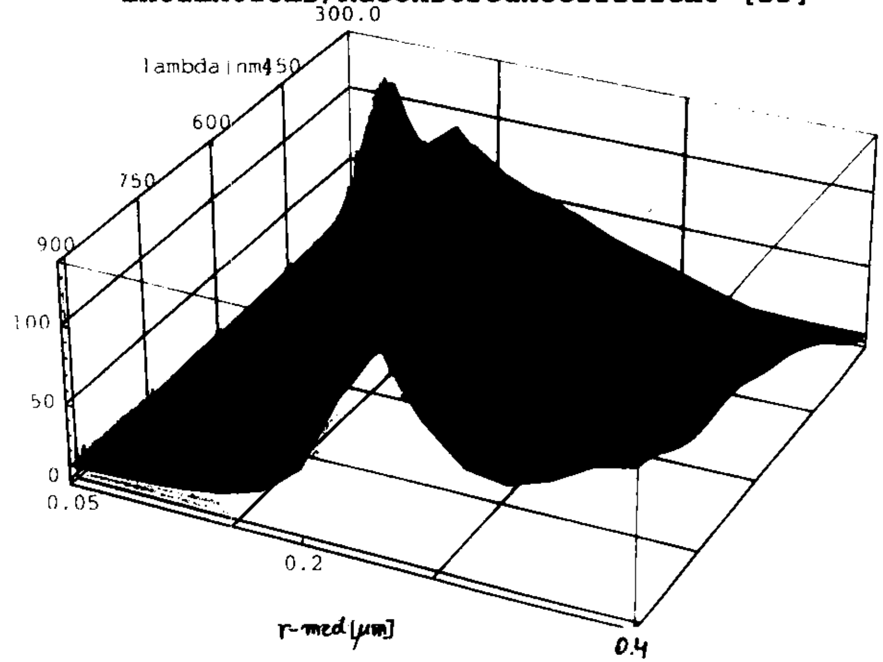

Properties of Raman scattering

frequency of incident light

frequency of j'th vibrational mode

zero point vibrational amplitude= $(h/8\pi^2\nu_j)^{1/2}$

$$\frac{d\sigma_j}{d\Omega} = \left(\frac{2\pi}{c}\right)^4 \frac{b_j^2(\nu_0 - \nu_j)^4}{[1 - \exp(-h\nu_j/kT)]} g_j \left(\alpha_j'^2 + \frac{7}{45}\gamma_j'^2\right)$$

trace and anisotropy of the polarizibility tensor

- Raman scattering cross section is about 1/1000 of Rayleigh crosss section !
- no angular dependance
- Raman shift is element specific

Raman Scattering

Vibrational-Rotational energy levels

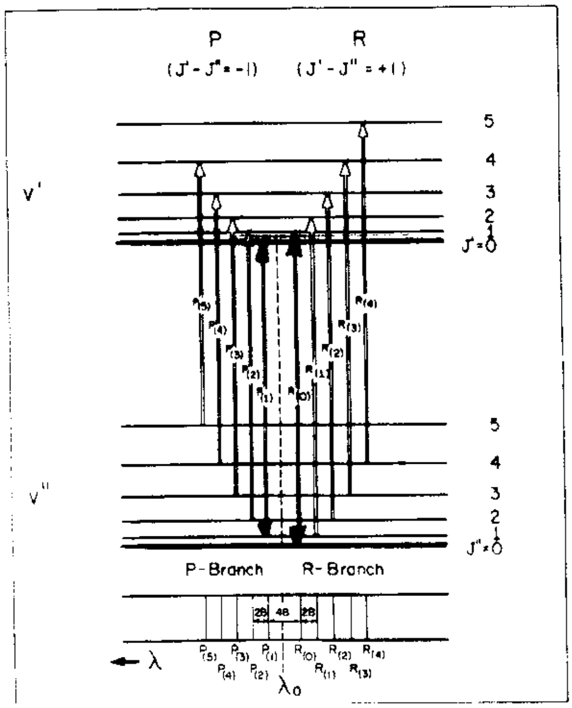

Raman spectrum of N_2

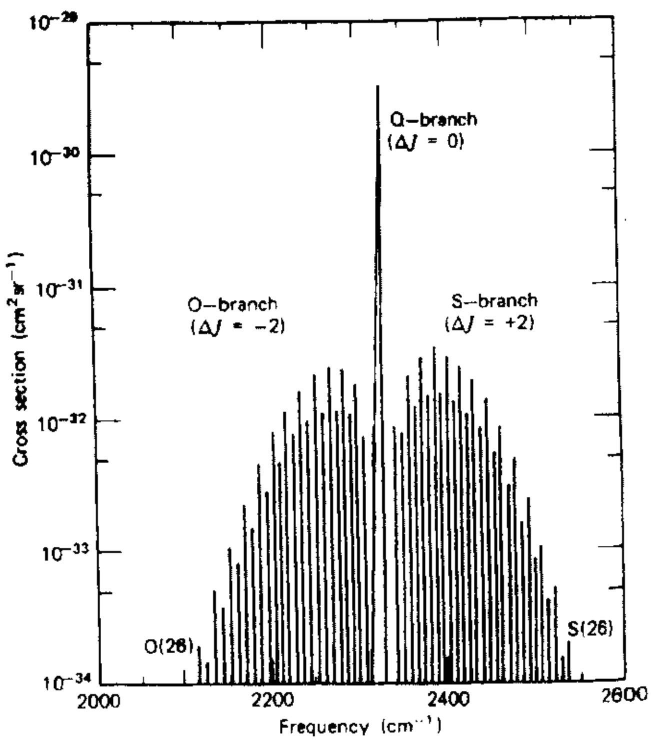

Calculation of the backscatter coefficient β^{aer}

$P(\lambda,z) = P_0 \cdot C(\lambda,z) \cdot A \cdot \frac{1}{z^2} \beta(\lambda,z) e^{-\int 2\alpha(\lambda,z) dz}$

1. **elastic Lidar signal:**

$$P_{\lambda_0} = \frac{\beta^{mol}_{\lambda_0} + \beta^{aer}_{\lambda_0}}{z^2} T_{\lambda_0} T_{\lambda_0} \qquad \text{with} \qquad T_{\lambda_0} = \exp\left\{ - \int_z \alpha^{aer}_{\lambda_0} + \alpha^{mol}_{\lambda_0} dz \right\} \qquad (1)$$

2. **Raman Lidar signal:**

$$P_{\lambda_R} = \frac{\beta^{N_2}_{\lambda_R}}{z^2} T_{\lambda_0} T_{\lambda_R} \qquad \text{with} \qquad T_{\lambda_R} = \exp\left\{ - \int_z \alpha^{aer}_{\lambda_R} + \alpha^{mol}_{\lambda_R} dz \right\} \qquad (2)$$

3. **definitions and assumptions:**

$$\beta^{N_2} \sim \beta^{mol}. \Rightarrow \quad R = \frac{\beta^{aer} + \beta^{mol}}{\beta^{mol}} \sim \frac{\beta^{aer}_{\lambda_0} + \beta^{mol}_{\lambda_0}}{\beta^{N_2}_{\lambda_R}}. \qquad \alpha^{aer}_{\lambda_R} = \alpha^{aer}_{\lambda_0}. \qquad (3)$$

4. **backscatter ratio:**

$$R = \frac{\beta^{aer} + \beta^{mol}}{\beta^{mol}} \sim \frac{P_{\lambda_0} T_{\lambda_R}}{P_{\lambda_r} T_{\lambda_0}} = \frac{P_{\lambda_0}}{P_{\lambda_R}} \exp\left\{ \int_z \left(\alpha^{mol}_{\lambda_0} - \alpha^{mol}_{\lambda_R} \right) dz \right\} \sim \frac{\beta^{aer}}{\beta^{mol}}. \qquad (4)$$

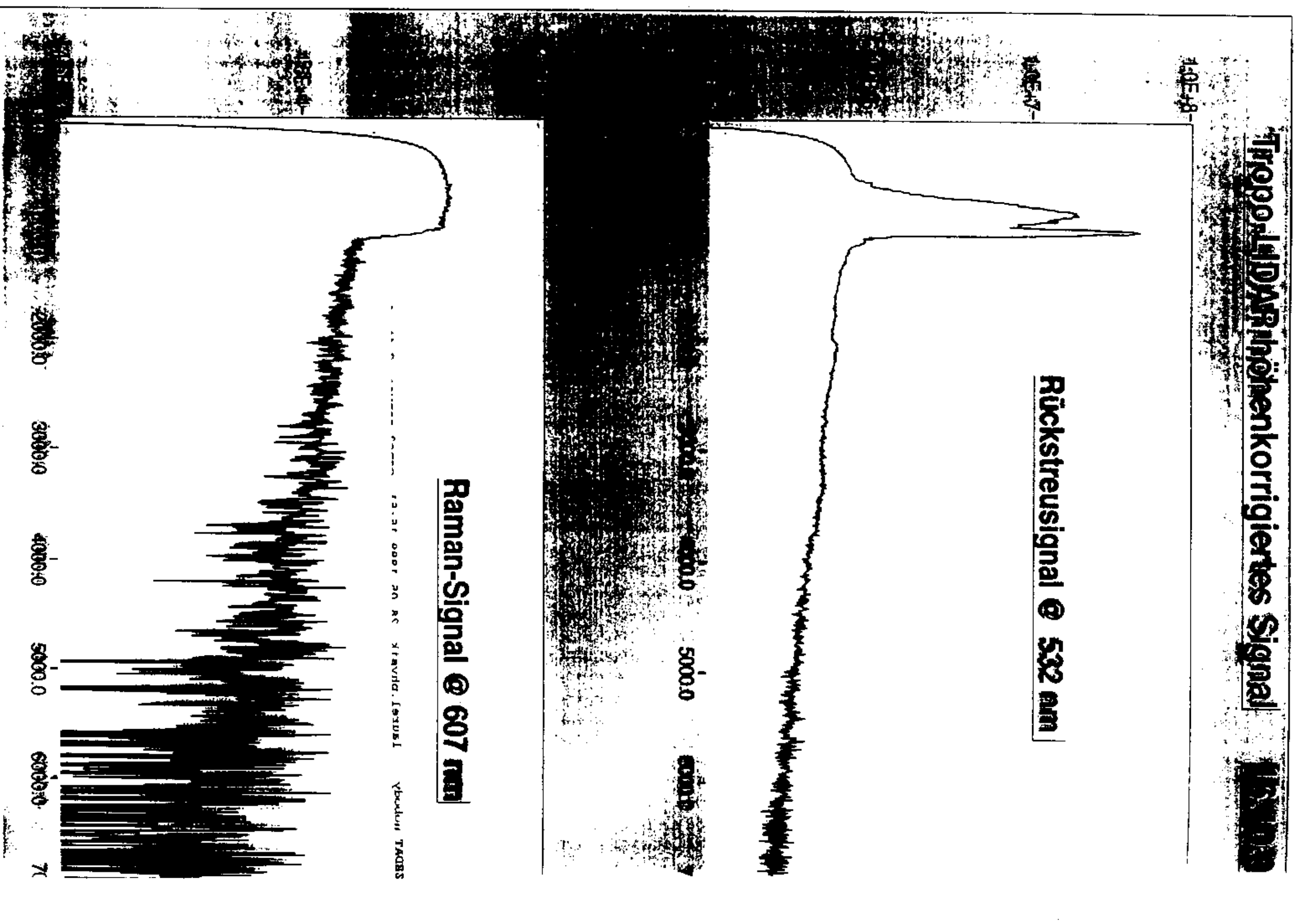

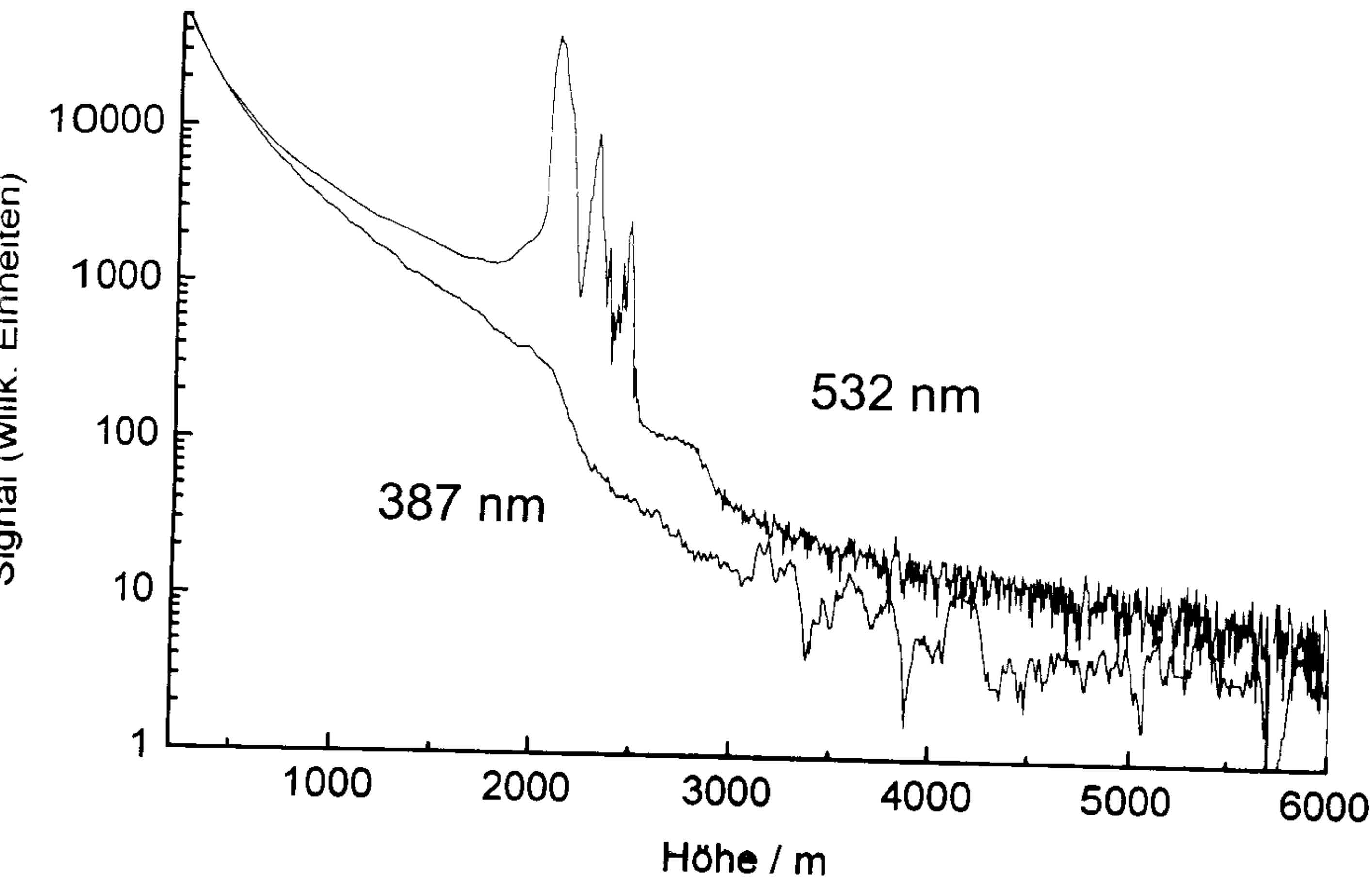

Theory II - Extinction calculation

1. **Raman extinction profile**

$$\alpha_{\lambda_0}^{aer}(z) = \frac{\frac{d}{dz}\left[\ln \frac{N(z)}{S_{Ram}(z)}\right] - \alpha_{\lambda_0}^{mol}(z) - \alpha_{\lambda_R}^{mol}(z)}{1 + \left(\frac{\lambda_0}{\lambda_R}\right)^k}$$

(Ansmann, 1992)

2. **Raman optical depth:**

$$\tau(z_b, z_t) = \frac{1}{2} \ln \left(\frac{S(z_b)N(z_t)}{S(z_t)N(z_b)}\right) - \frac{1}{2}\int_{z_b}^{z_t} \left(\alpha_{\lambda_0}^{mol}(z) + \alpha_{\lambda_R}^{mol}(z)\right) dz$$

AWI

Koldewey Station, Ny-Aalesund, Svalbard

78.9 N, 11.9 E

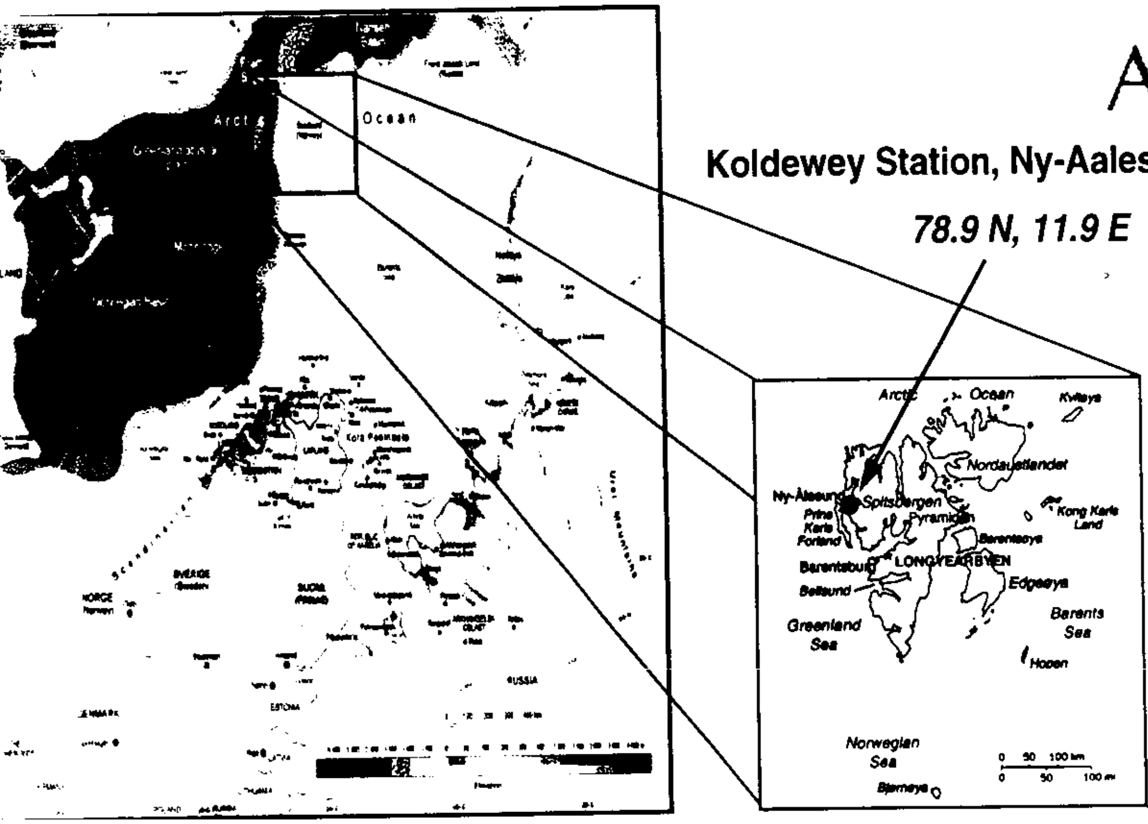

Sensitivity I - realistic example

haze layer: 2-3 km
integrated time: 1 h
Kaiser Filter
$\alpha^{Aer} = 7 \cdot 10^{-5} \mathrm{m}^{-1}$
Lidar Ratio: 40sr

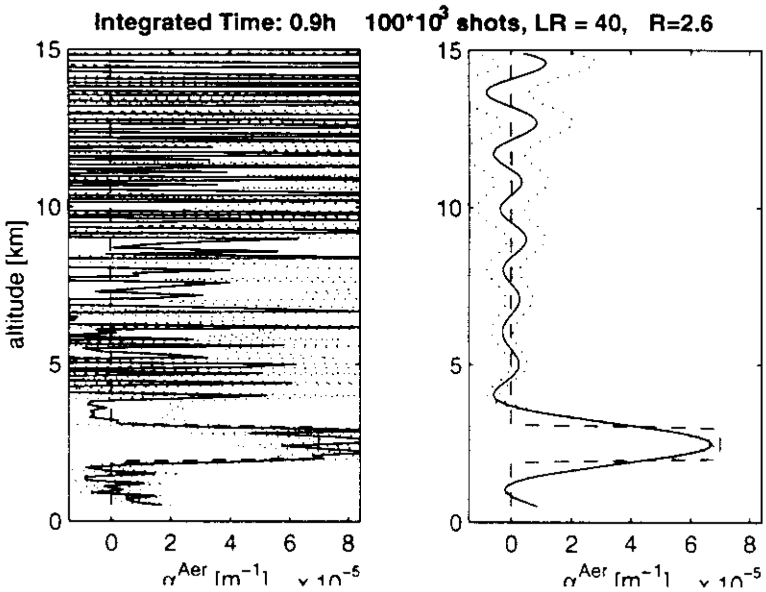

Principle of Aerosol Extinction measurement during ASTAR2000

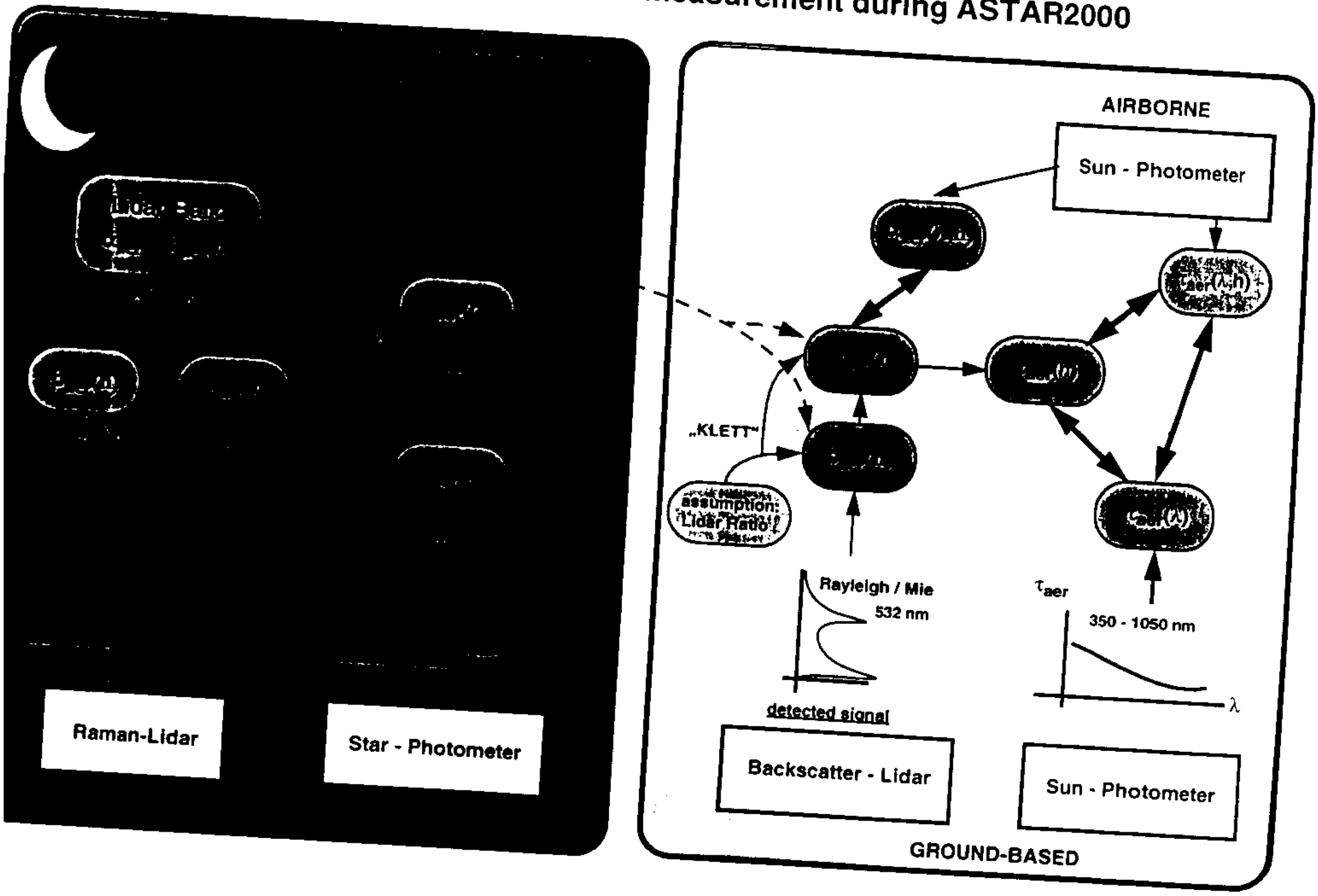

AWI Tropospheric Aerosol Raman Lidar

Experimental Setup 1999/2000, Ny-Aalesund, Spitsbergen 78.9 N, 11.9 E

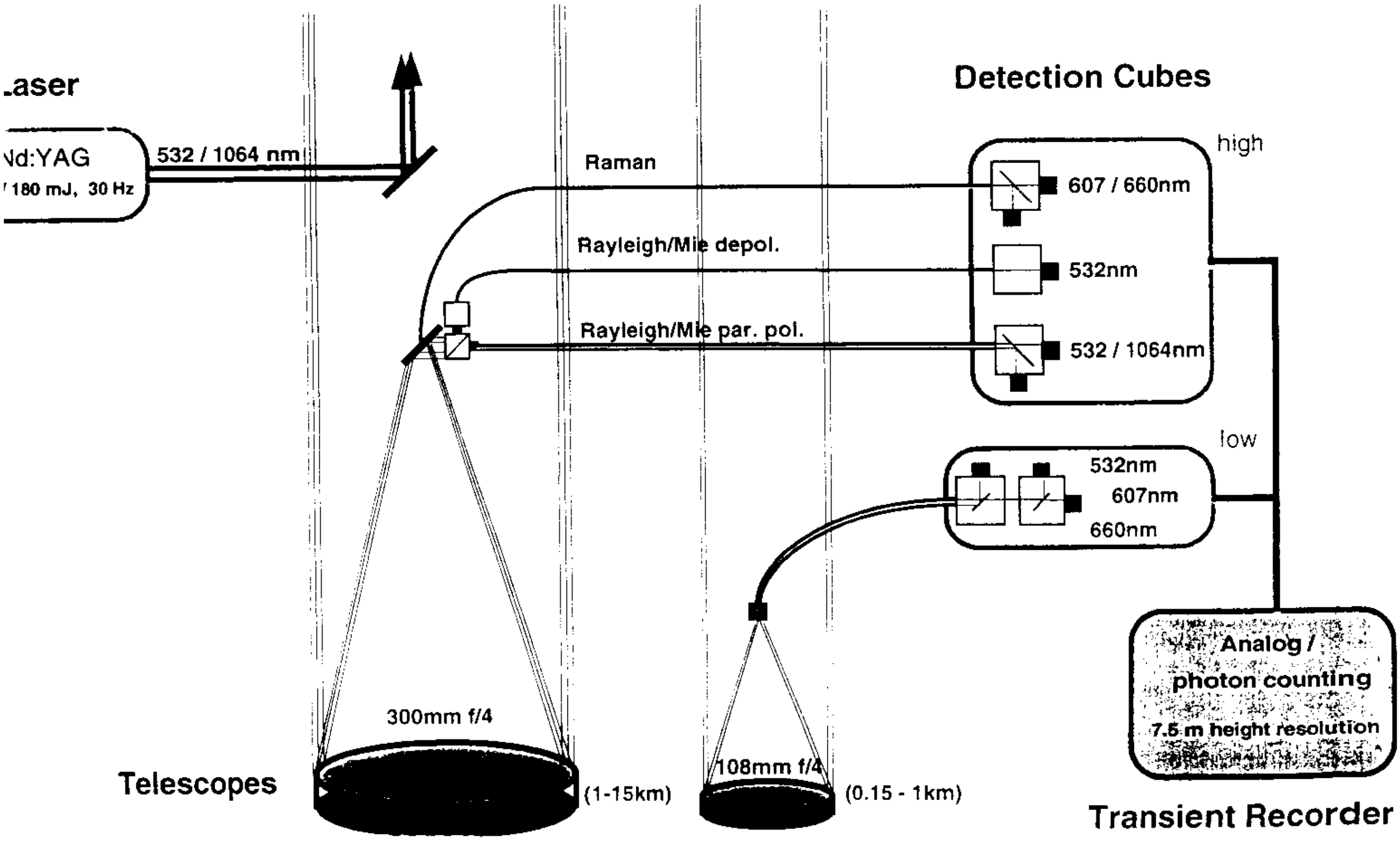

extinction coefficient

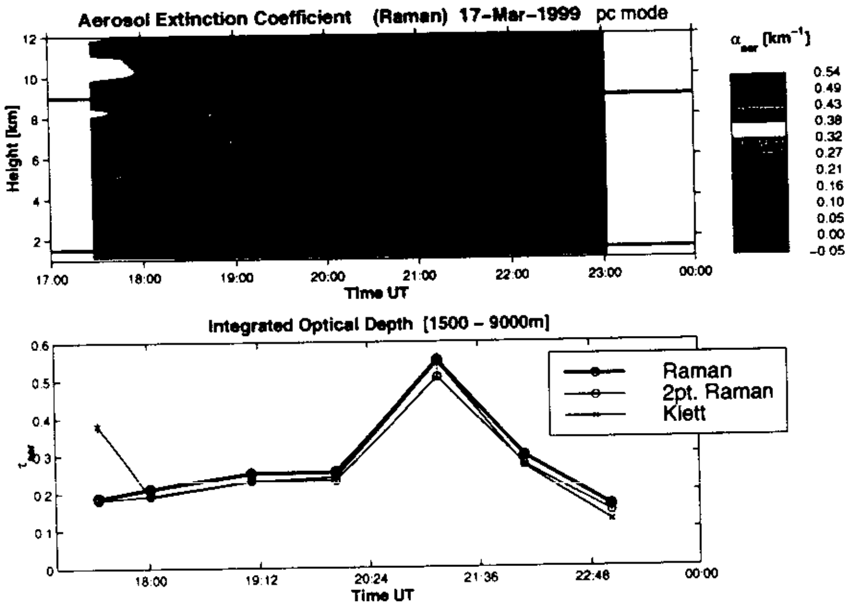

profiles

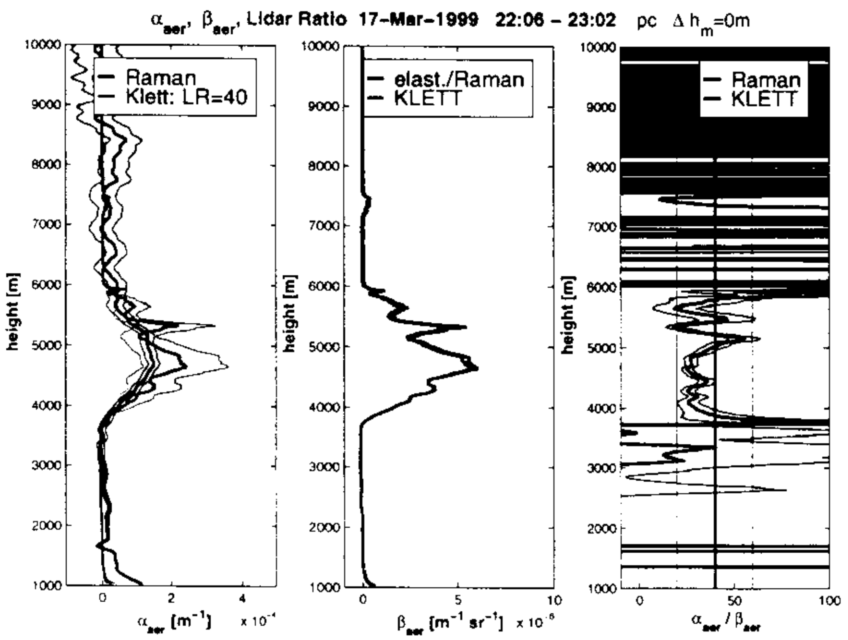

High spectral resolution lidar

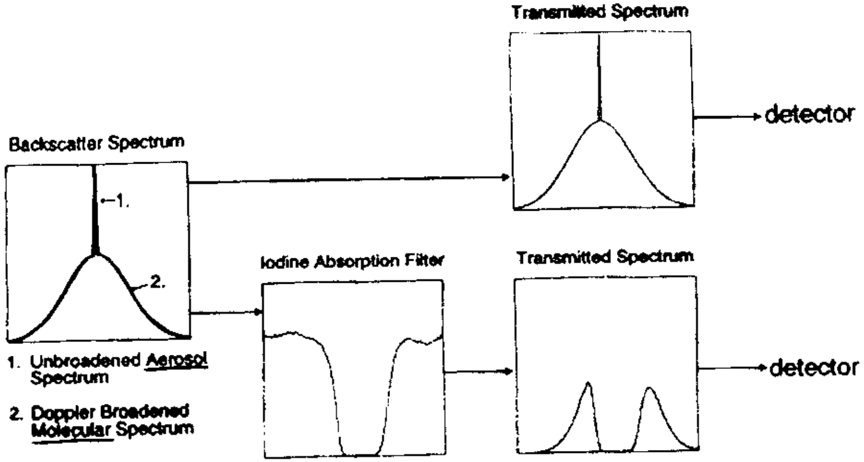

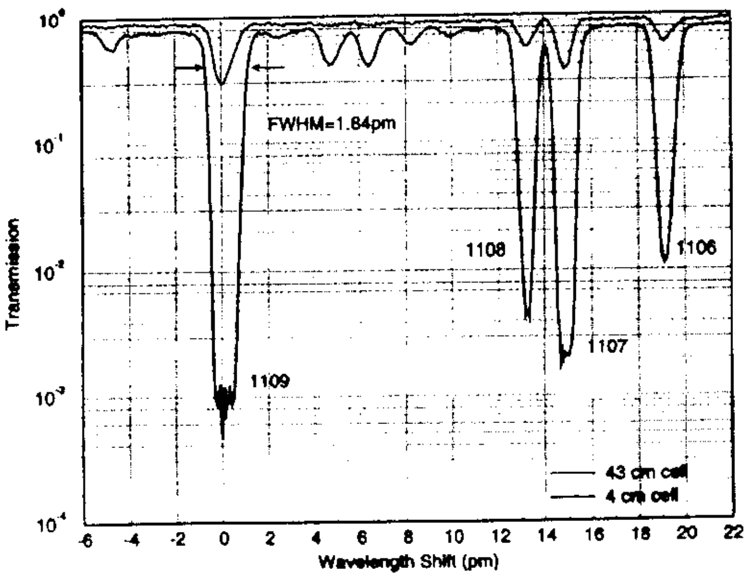

Optical depth: LIDAR - Photometer

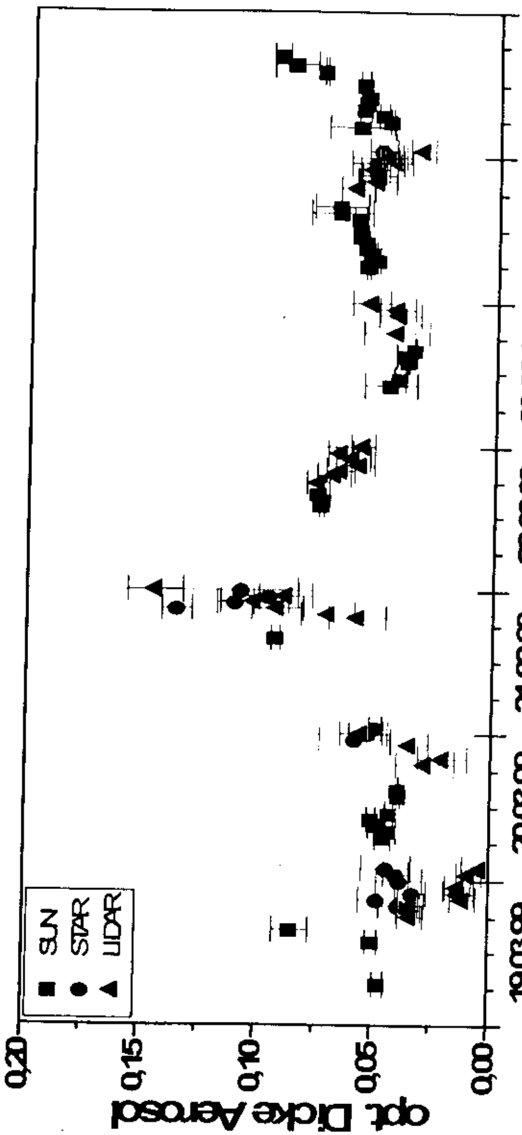

Multicomponent Analysis by Raman Lidar

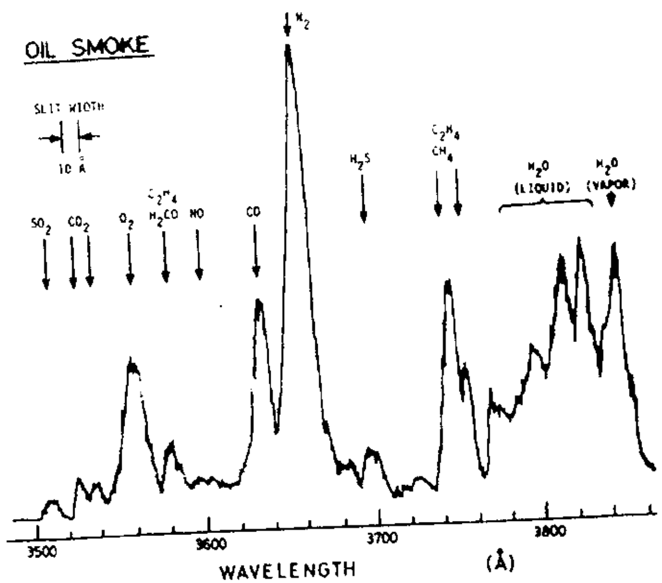

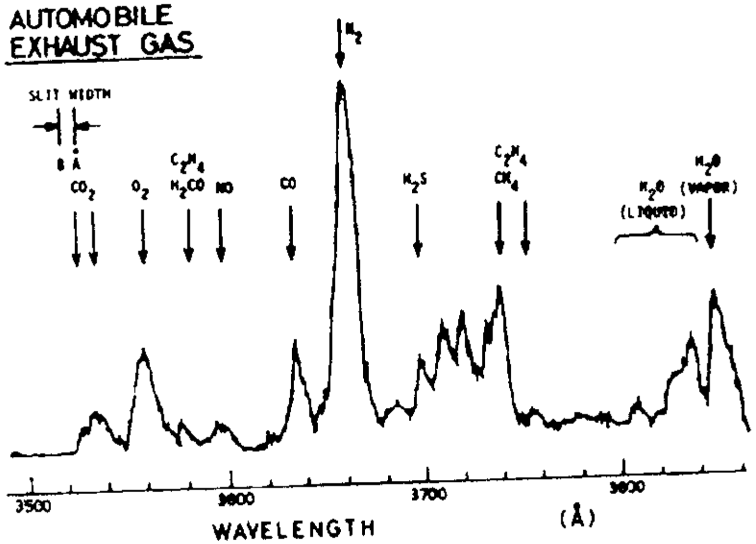

Multicomponent Analysis using Raman Lidar

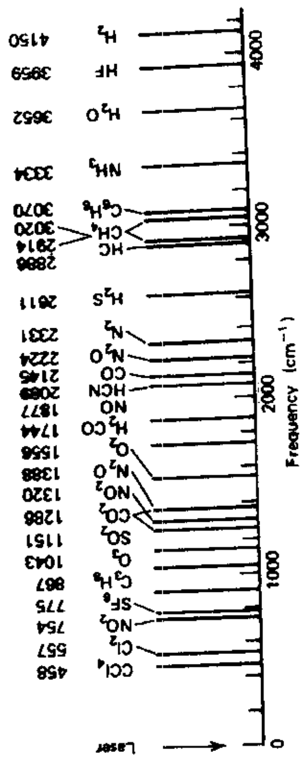

Frequency shifts of vibrational Raman lines

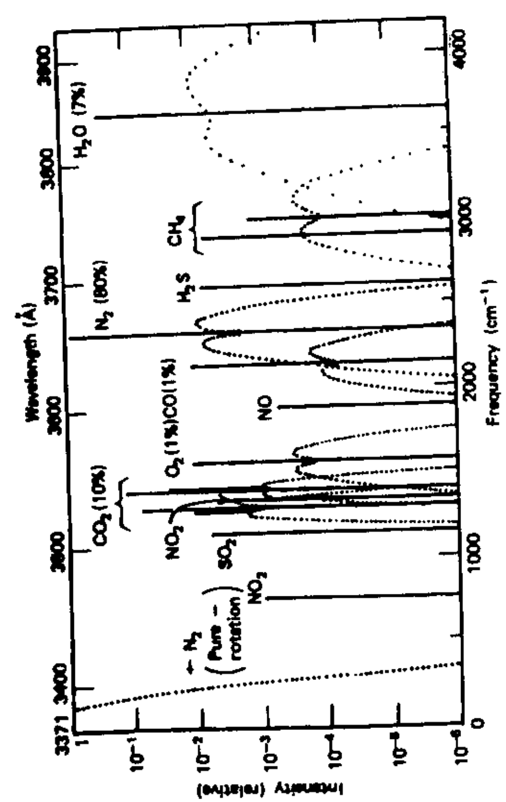

Multicomponent Raman spectrum

Temperature Measurement by Rayleigh Lidar

above 25-30 km:

Lidar signal depends on air density only

$$n_R(r) \propto P(r)r^2$$

in hydrostatic equilibrum:

integration of density profile yields a (relative) pressure profile

$$p(r) = p(r_o) - \int_r^{r_o} n_R(r')Mg(r')dr'$$

Using pV = N R T the temperature can be retrieved by starting at r_0 (typ. 55-65 km) and downward integration:

$$T(r) = T(r_o)\frac{r_o^2 P(r_o)}{r^2 P(r)} + \frac{M}{k_B}\frac{\int_{r_o}^{r} r'^2 P(r')g(r')dr'}{r^2 P(r)}$$

H_2O-Raman Profile

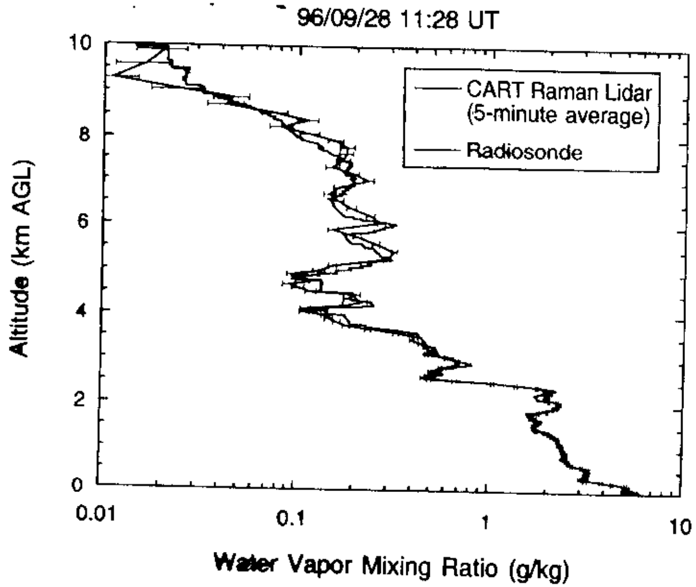

Molecule	ν_j (cm^{-1})	λ_r (Å)	$d\sigma/d\Omega$ ($cm^2 str^{-1}$)	References
CCl_4	459	3424	26×10^{-30}	[23]
$NO_2(\nu_2)$	754	3457	24	[27]
SF_6	775	3461	12	[23]
$C_6H_6(\nu_2)$	991	3487	44	[23, 27]
SO_2	1151.5	3508	17	[24-26]
$CO_2(2\nu_2)$	1285	3525	3.1	[23, 26]
$NO_2(\nu_1)$	1320	3528	51	[27]
$CO_2(\nu_1)$	1388	3537	4.2	[23-26]
O_2	1556	3559	4.6	[23, 26]
$C_2H_4(\nu_2)$	1623	3566	3.3(Q)	[23-26]
NO	1877	3600	5.4(Q)	[23]
CO	2145	3635	1.5	[24, 26]
N_2	2330.7	3659	3.6	[23-26]
			3.5	[23, 25]
H_2S	2611	3697	2.8(Q)	[23-25]
$CH_3OH(\nu_2)$	2846	3728	19	[23, 24]
$CH_4(\nu_1)$	2914.2	3739	14	[23, 27]
C_2H_5OH	2943	3742	21	[23, 25, 27]
$CH_3OH(2\nu_6)$	2955	3744	19	[23, 27]
$CH_4(\nu_3)$	3017	3752	7.5	[23, 27]
$C_2H_4(\nu_1)$	3020	3753	14	[23, 27]
$C_6H_6(\nu_1)$	3070	3760	16(Q)	[23]
NH_3	3334	3798	30	[23, 27]
H_2O	3651.7	3844	11	[23]
H_2	4160.2	3922	7.8(Q)	[25, 27]
			8.7	[23, 26]

Rotations-Raman Spektrum

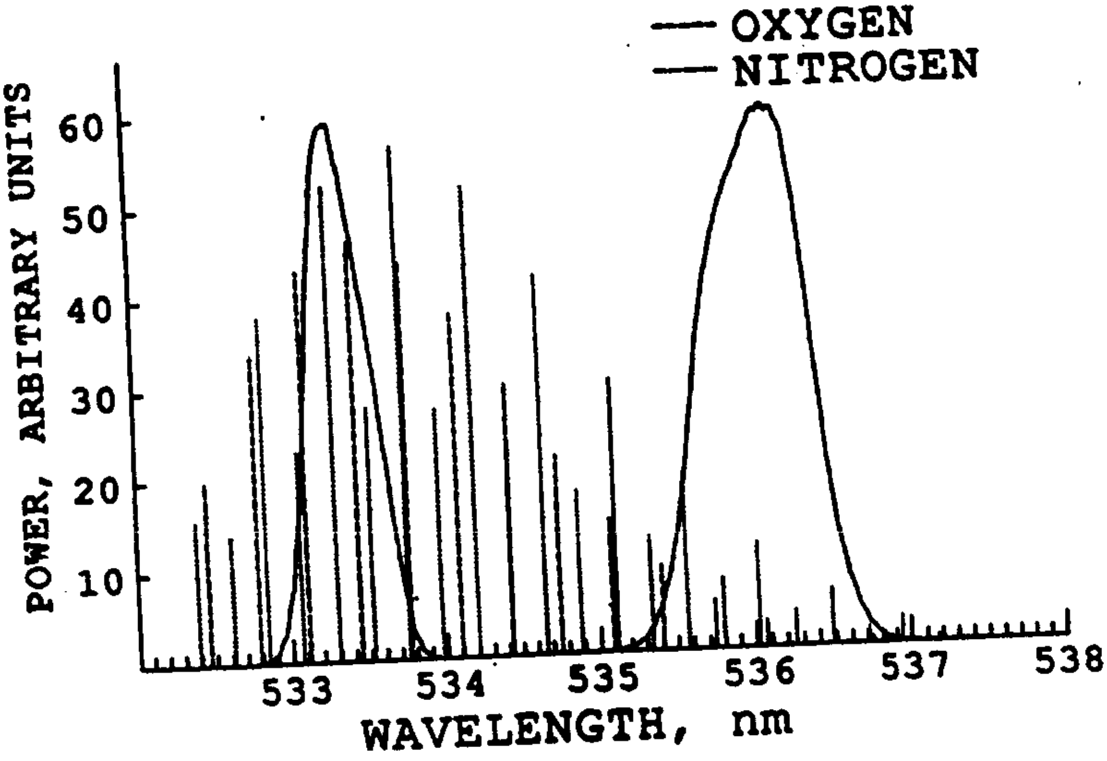

Temperature Measurement by Rayleigh Lidar

Comparison of balloon and lidar measurement

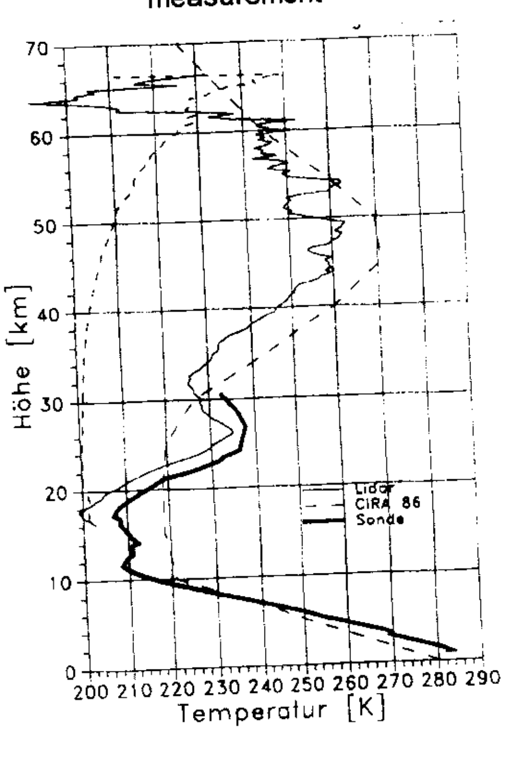

Temp. error (start height r_0)

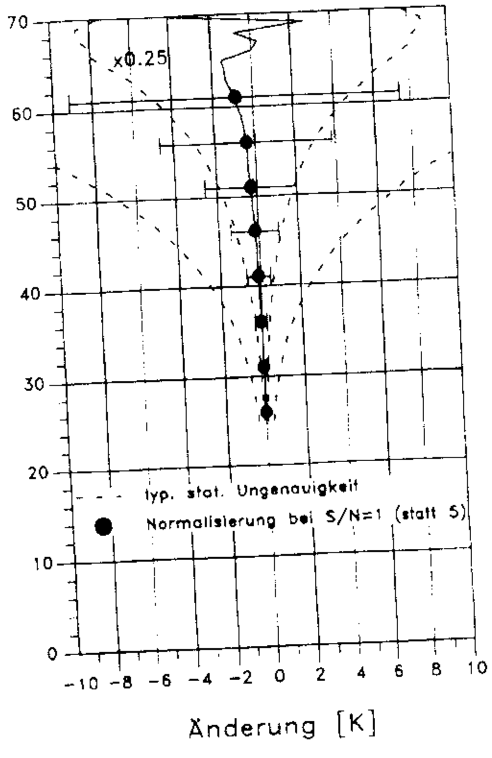

Total temp. error

height/km	Temp/K
25	0.4
30	0.7
35	1.4
40	2.5
45	4.2
50	6.7
55	11
60	18
65	30

Rotations-Raman Spektrum
Rohdaten der CCD Kamera

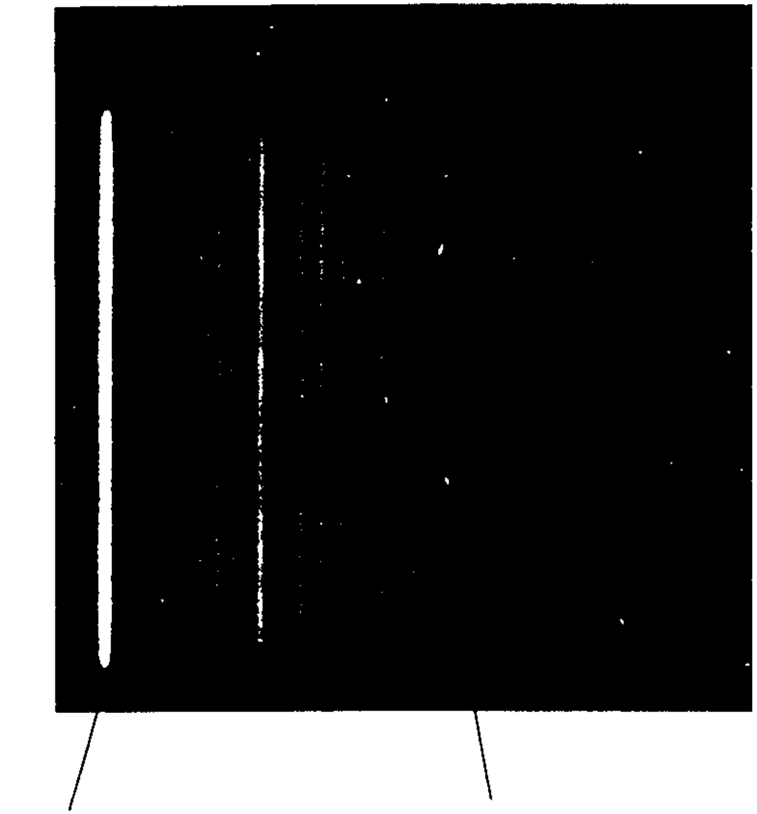

Hochaufgelöste Messung der Rotations-Raman Linien

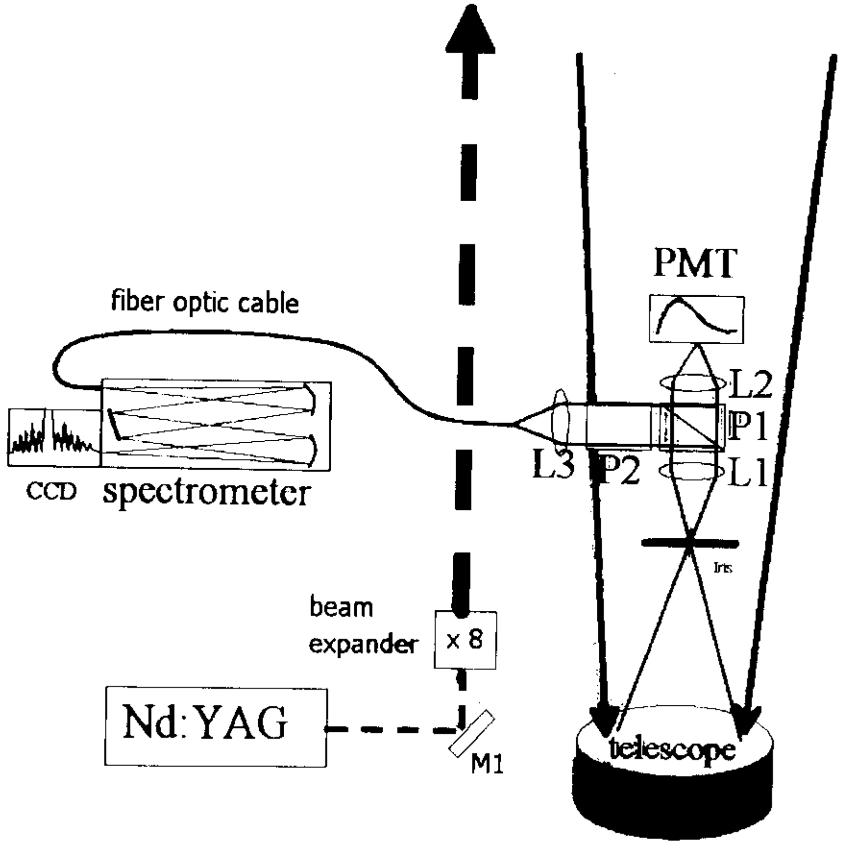

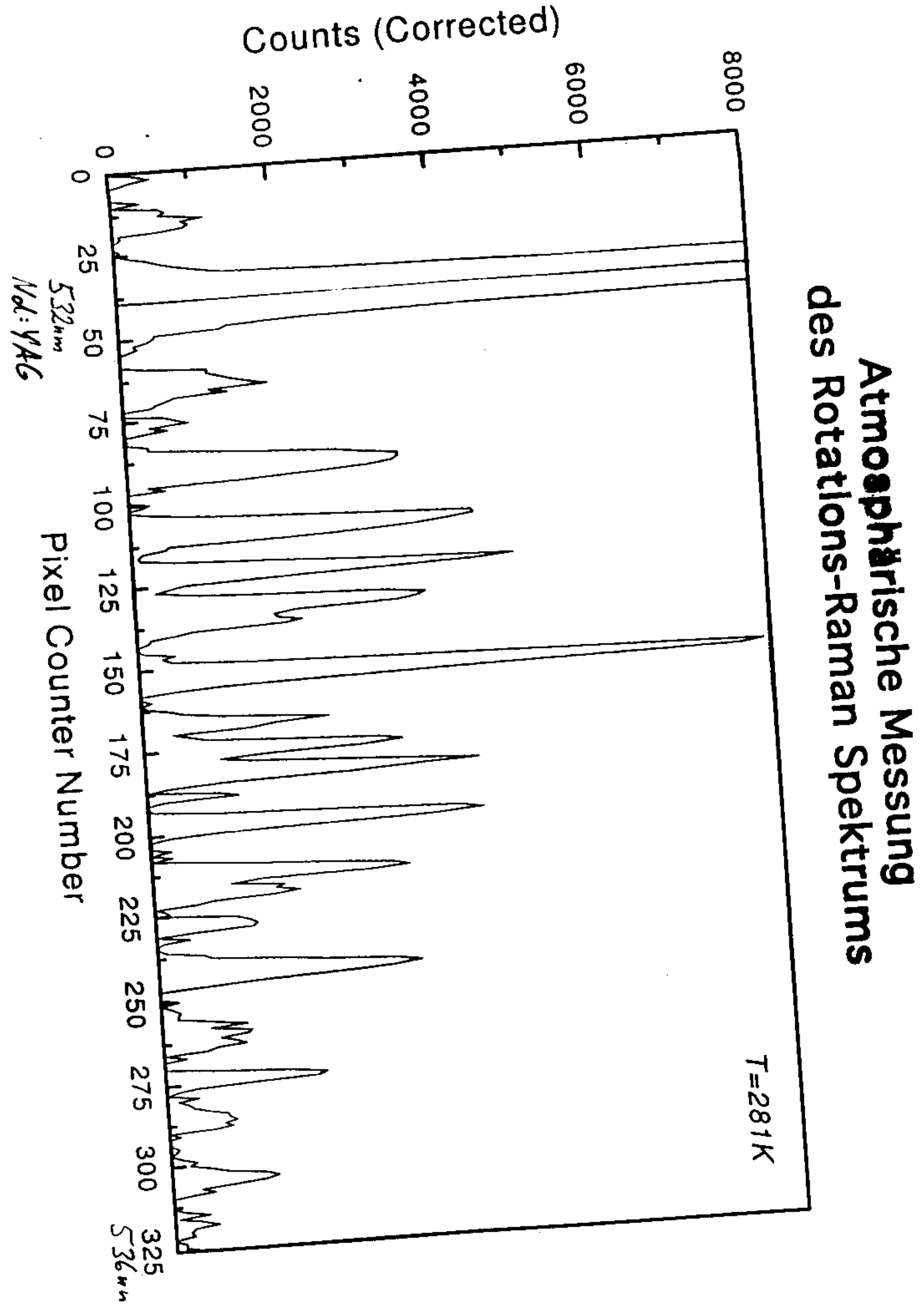

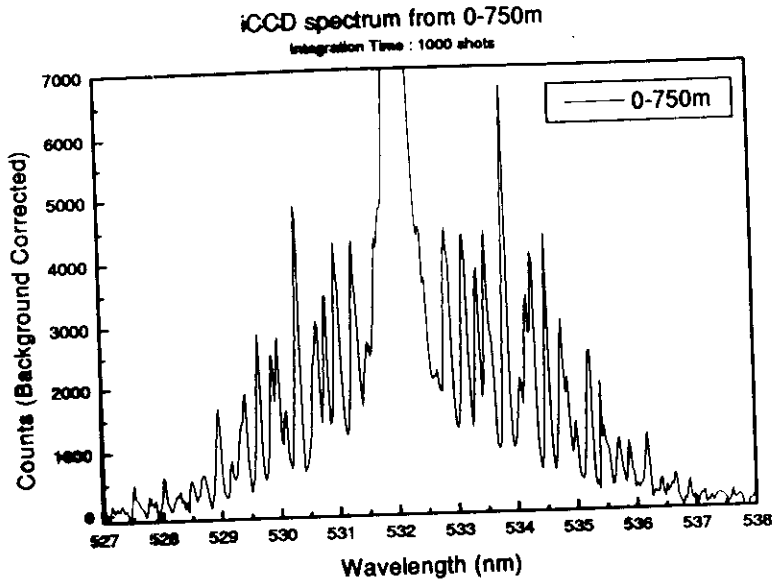

Figure 4 : View of spectrum from 0-750 m showing the wings of the elastic scattering as a baseline underneath the Raman spectrum.

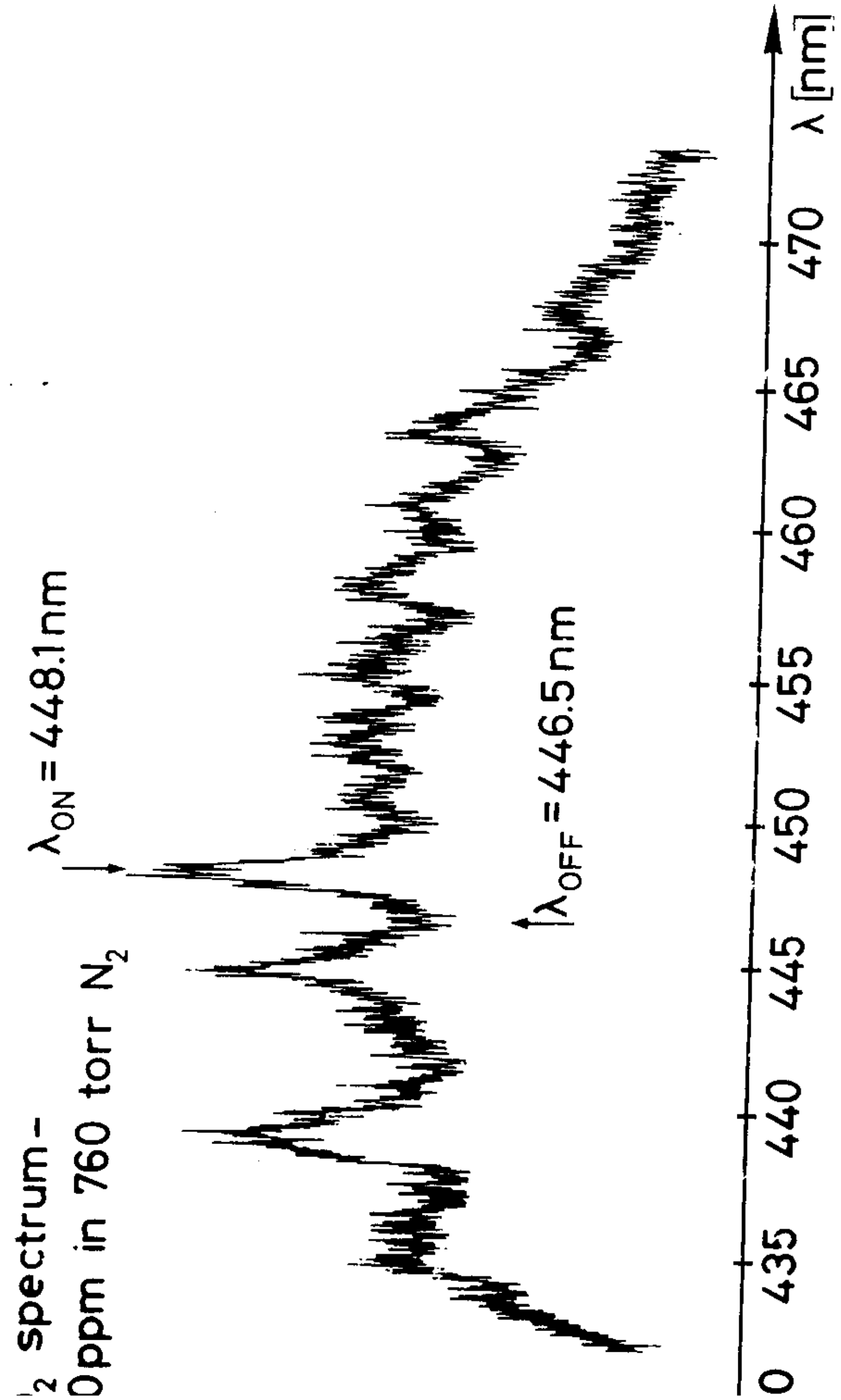

Trace gas measurements by lidar

1. The DIAL technique
   - derivation of the DIAL equation
   - detectable species/usable wavelengths
   - cross sensitivity
   - experimental examples/measurements

2. Wind lidar
   - Heterodyne technique
   - edge technique
   - volume scanning lidar

3. Femtosecond „white light“ lidar
   - generation of white light in the atmosphere
   - nonlinear effects
   - experimental setup
   - aerosol and trace gas measurements

Derivation of the DIAL equation

divide signals of λ_{on} und λ_{off}:

$$\frac{P(\lambda_{on})}{P(\lambda_{off})} = \frac{C(\lambda_{on},R)\cdot P_L(\lambda_{on})\cdot\beta(\lambda_{on},R)\cdot\exp\left(-2\int_0^R \alpha(\lambda_{on},r)\cdot dr\right)}{C(\lambda_{off},R)\cdot P_L(\lambda_{off})\cdot\beta(\lambda_{off},R)\cdot\exp\left(-2\int_0^R \alpha(\lambda_{off},r)\cdot dr\right)}$$

„simple solution":

$$\frac{P(\lambda_{on})}{P(\lambda_{off})} = C\cdot e^{-2\int_0^R \alpha(\lambda_{on},r)-\alpha(\lambda_{off},r)\,dr}$$

$$\ln\left(\frac{P(\lambda_{on})}{P(\lambda_{off})}\right) = \ln C + \left(-2\int_0^R \alpha(\lambda_{on},r)-\alpha(\lambda_{off},r)\right)dr$$

$$\frac{\partial}{\partial r}\ln\left(\frac{P(\lambda_{on})}{P(\lambda_{off})}\right) = -2\left(\alpha(\lambda_{on},r)-\alpha(\lambda_{off},r)\right)$$

complete solution:

$$N(R) = -\frac{1}{2\cdot\Delta\sigma}\left[\underbrace{\frac{\partial}{\partial R}\ln\frac{P(R,\lambda_{on})}{P(R,\lambda_{off})}}_{A} - \underbrace{\frac{\partial}{\partial R}\ln\frac{\beta(\lambda_{on},R)}{\beta(\lambda_{off},R)}}_{B} + \underbrace{2(\alpha_{m,a}(\lambda_{on},R) - \alpha_{m,a}(\lambda_{off},R}_{C}\right.$$

DIAL- Methode

LIDAR-Gleichung: $P(\lambda,r) = C\frac{A}{r^2}\beta(r)\,exp\left[-2\int_0^r \alpha(r)\,dr\right]$

$$N(r) = -\frac{1}{2\Delta\sigma}\left[\frac{d}{dr}ln\left(\frac{P(\lambda_{on},r)}{P(\lambda_{off},r)}\right) - \frac{d}{dr}ln\left(\frac{R(\lambda_{on},r)}{R(\lambda_{off},r)}\right)\right]$$

- ln (signal)

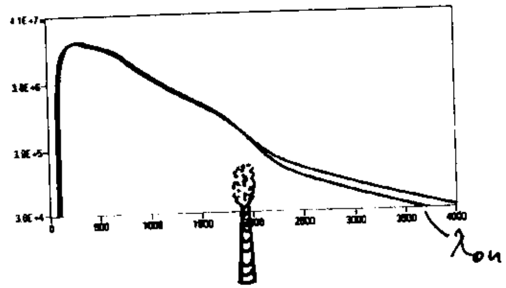

- $\frac{ln(\lambda_{on})}{ln(\lambda_{off})}$

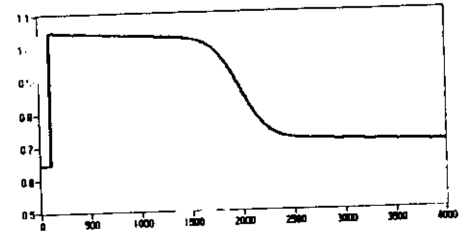

$-\frac{\partial}{\partial r}\frac{ln(\lambda_{on})}{ln(\lambda_{off})}$

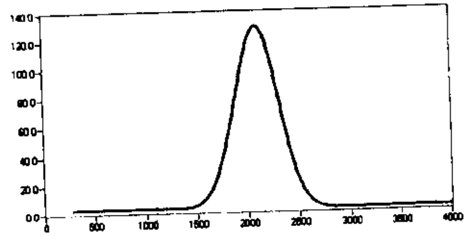

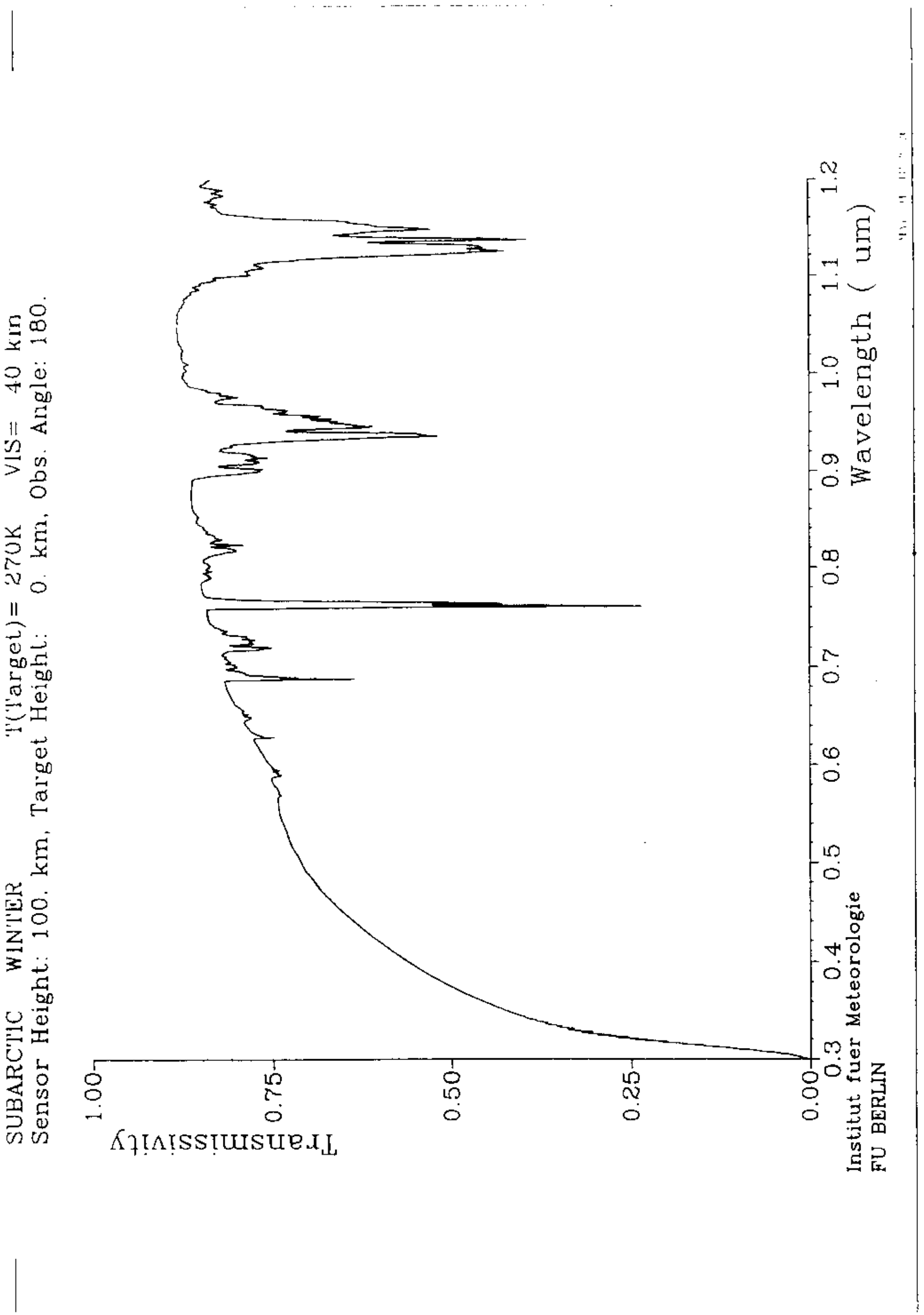

DIAL absorption cross section for different trace gases

Molecule		Wavelength	Laser (Examples)	Absorption cross s- 10^{-18} cm²
Nitric oxide, NO		226.8 nm	Dye	4.6
Benzene, C_6H_6		252.9 nm	Dye	5.7
Mercury, Hg		253.65 nm	Dye	3.3×10^4
Toluene, C_7H_8		266.9 nm	Dye, Ti:Sa	2.8
Ozone, O_3		266.0 nm	Dye, KrF, Nd:YAG-	
	UV	289.0 nm	IV + Raman cell	9.49
		299.0 nm	Ti:Sa	1.59
			Ce:LiSAF	0.42
Formaldehyde, CH_2O		286.5	Dye, Ti:Sa	0.068
Sulfur dioxide, SO_2		300.0 nm	Dye, Ti:Sa	1.3
Chlorine, Cl_2		330 nm	Dye, Ti:Sa	0.26
			XeCl + Raman cell	
Nitrous acid, HONO		354.0 nm	Dye, Ti:Sa	0.50
Nitrogen dioxide, NO_2	Vis	448.1 nm	Dye	0.69
Methane, CH_4		3.270 μm	OPO	2.0
		3.391 μm		0.6
Propane, C_3H_8		3.391 μm	OPO	0.8
Hydrogen chloride, HCl		3.636 μm	DF, OPO	0.20
Methane, CH_4		3.715 μm	DF, OPO	0.002
Sulfur dioxide, SO_2	NIR	3.984 μm	DF, OPO	0.42
Carbon monoxide, CO		4.709 μm	CO_2	2.8
		4.776 μm		0.8
Nitric oxide, NO		5.215 μm	CO	0.67
		5.263 μm	CO_2	0.6
Propylene, C_3H_6		6.069 μm	CO	0.09
1,3-Butadiene, C_4H_6		6.215 μm	CO	0.27
Nitrogen dioxide, NO_2		6.229 μm	CO	2.68
Sulfur dioxide, SO_2		9.024 μm	CO_2	0.25
Freon-11, CCl_3F		9.261 μm	CO_2	1.09
Ozone, O_3		9.505 μm	CO_2	0.45
		9.508 μm		0.9
Fluorocarbon-113, $C_2Cl_3F_3$		9.604 μm	CO_2	0.77
Benzene, C_6H_6		9.621 μm	CO_2	0.07
MMH, $CH_3N_2H_3$		10.182 μm	CO_2	0.06
Ethyl-mercaptan, C_2H_5SH		10.208 μm	CO_2	0.02
Chloroprene, C_4H_5Cl	FIR	10.261 μm	CO_2	0.34
Monochloroethane, C_2H_5Cl		10.275 μm	CO_2	0.12
Ammonia, NH_3		10.333 μm	CO_2	1.0
Ethylene, C_2H_4		10.533 μm	CO_2	1.19
Sulfur hexafluoride, SF_6		10.551 μm	CO_2	30.3
Trichloroethylene, C_2HCl_3		10.591 μm	CO_2	0.49
1,2-Dichloroethane, $C_2H_4Cl_2$		10.591 μm	CO_2	0.02
Hydrazine, N_2H_4		10.612 μm	CO_2	0.18
Vinyl chloride, C_2H_3Cl		10.612 μm	CO_2	0.33
UDMH, $(CH_3)_2N_2H_2$		10.696 μm	CO_2	0.08
Fluorocarbon-12 (Freon-12), CCl_2F_2		10.719 μm	CO_2	1.33
Perchloroethylene, C_2Cl_4		10.742 μm	CO_2	0.18
1-Butene, C_4H_8		10.787 μm	CO_2	0.13
Perchloroethylene, C_2Cl_4		10.834 μm	CO_2	1.14
Fluorocarbon-11 (Freon-11), CCl_3F		11.806 μm		4.4
Acethylene, C_2H_2		13.890 μm		9.2

Difficulties of DIAL measurements

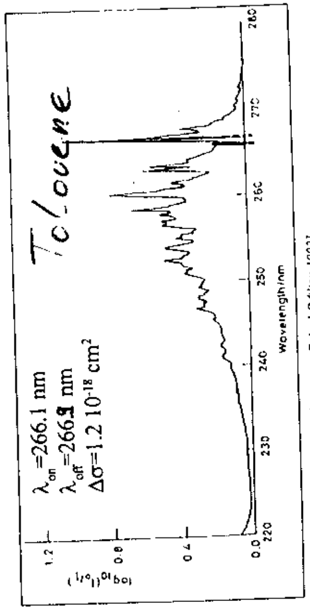

Abb. 19: Absorptionsspektrum von Toluol [Milton 1992]

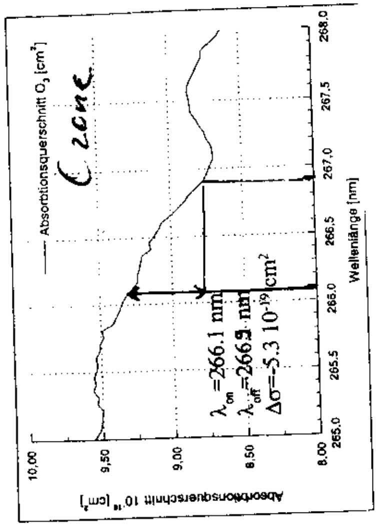

- cross sensitivity of different trace gases especially in the UV
- inhomogenous aerosol loading induce errors due to $\frac{\partial}{\partial R}\ln\frac{\beta(\lambda_{on},R)}{\beta(\lambda_{off},R)}$
- very good signal to noise ratio and signal smoothing required to avoid fluctuations of the derivative $\left|\frac{\partial}{\partial R}\ln\frac{P(R,\lambda_{on})}{P(R,\lambda_{off})}\right|$
- very sensitive to misalignment, especially in the geometrical overlap region

Photomultipliers

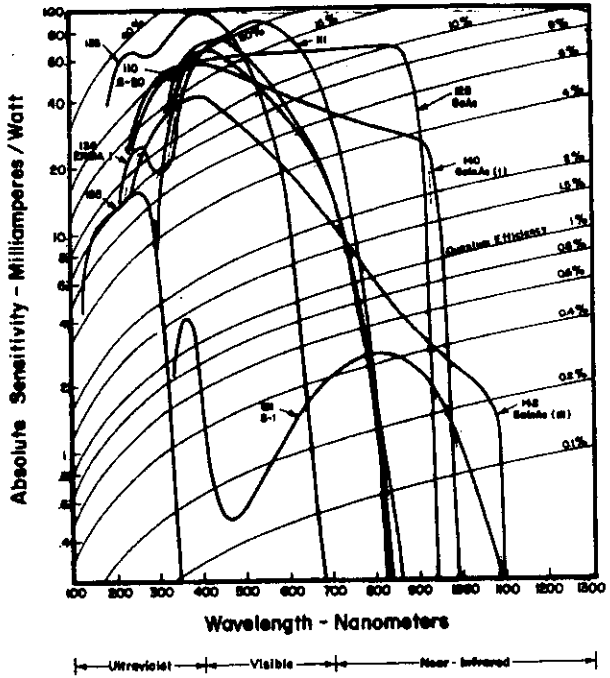

Photoconductors and photodiodes

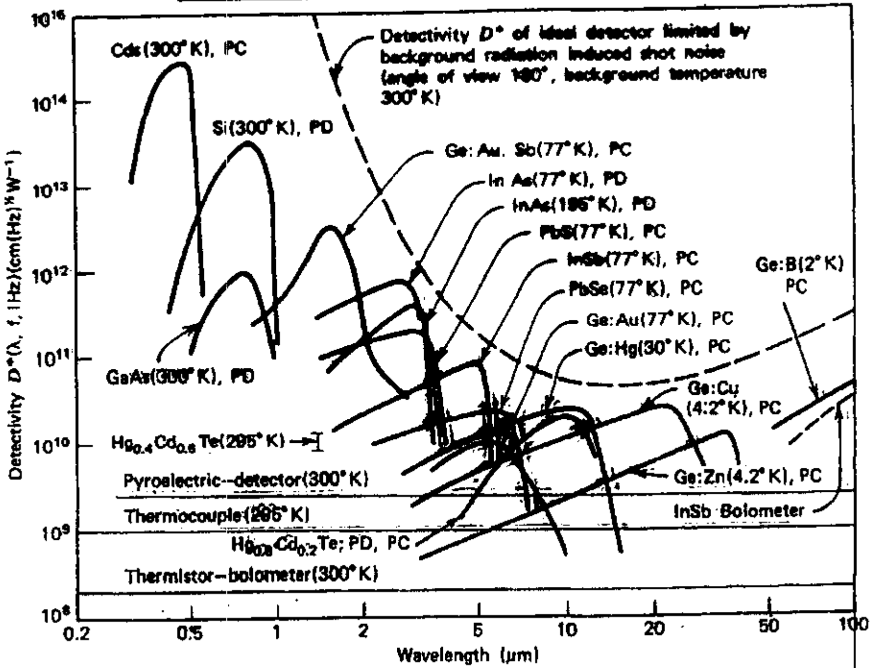

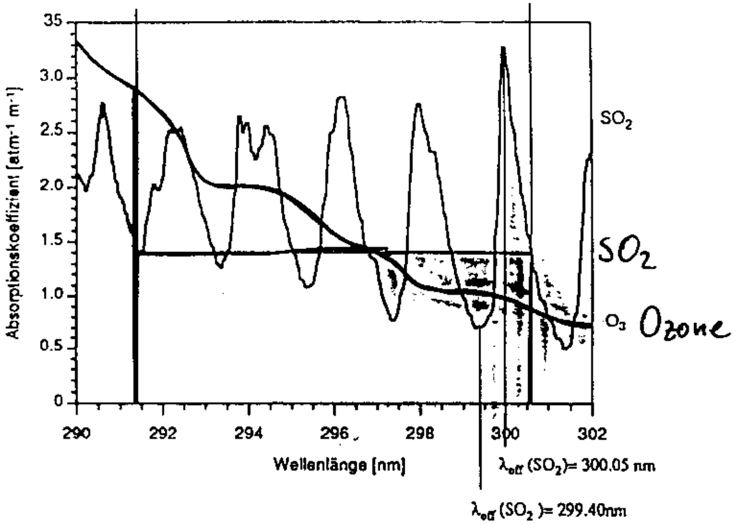

Abb. 3.2.3: Absorptionspektren von SO_2 und Ozon im Vergleich. Bei den ausgewählten Wellenlängen für Ozon hat SO_2 den gleichen Absorptionskeffizient. Ozon-Spektrum von M. Griggs [11], SO_2-Spekrum von D.J. Brassington [8]

3.1. Verwendete Absorptionsbanden SO_2

Für den Nachweis des SO_2 wird eine zentrale Vibrationsbande aus den sogenannten ersten erlaubten Absorbtionsband benutzt, das sich von 240 bis 330 nm erstreckt. Die Vergleichswellenlänge λ_{off} ist ein Minimum zwischen benachbarten Absorptionsbanden. Das 1. erlaubte Band wird nach

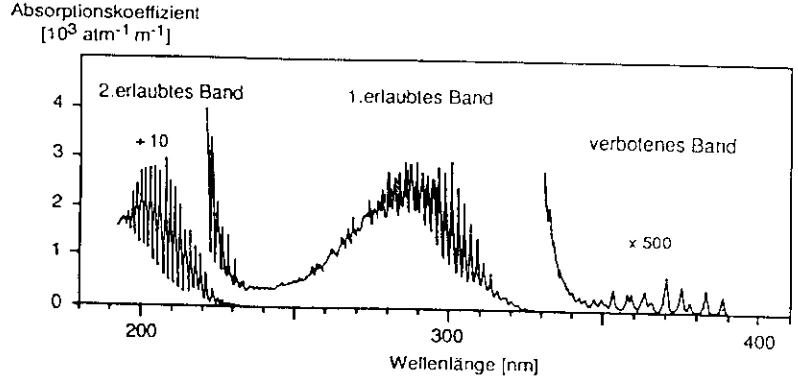

Abb. 3.1.2: Absorptionsspektrum von SO_2 im UV-Bereich. Im sichtbaren Bereich gibt es keine Absorption. Quelle: S.J. Streickler & Daniel B. Howell, 1968 [9]

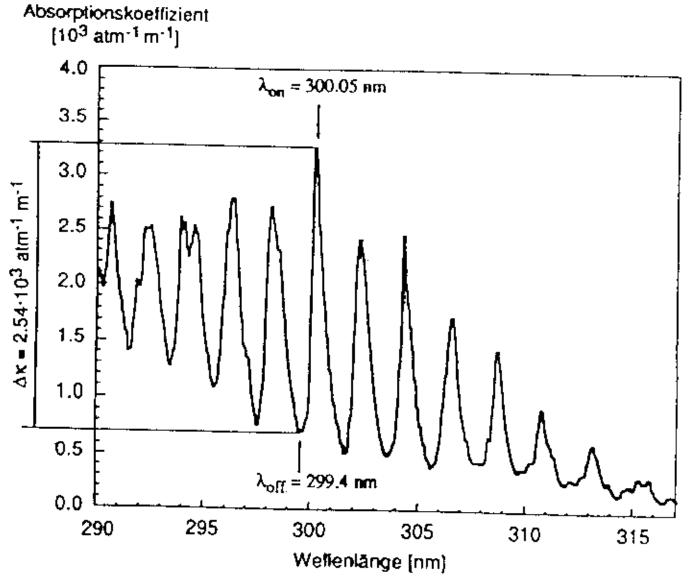

Abb. 3.1.2: Ausschnitt aus dem 1. erlaubten Band von SO2 und die vom LIDAR benutzten Wellenlängen. Quelle: D.J. Brassington 1981 [8]

Tropo-LIDAR Charité, Berlin: Set-Up

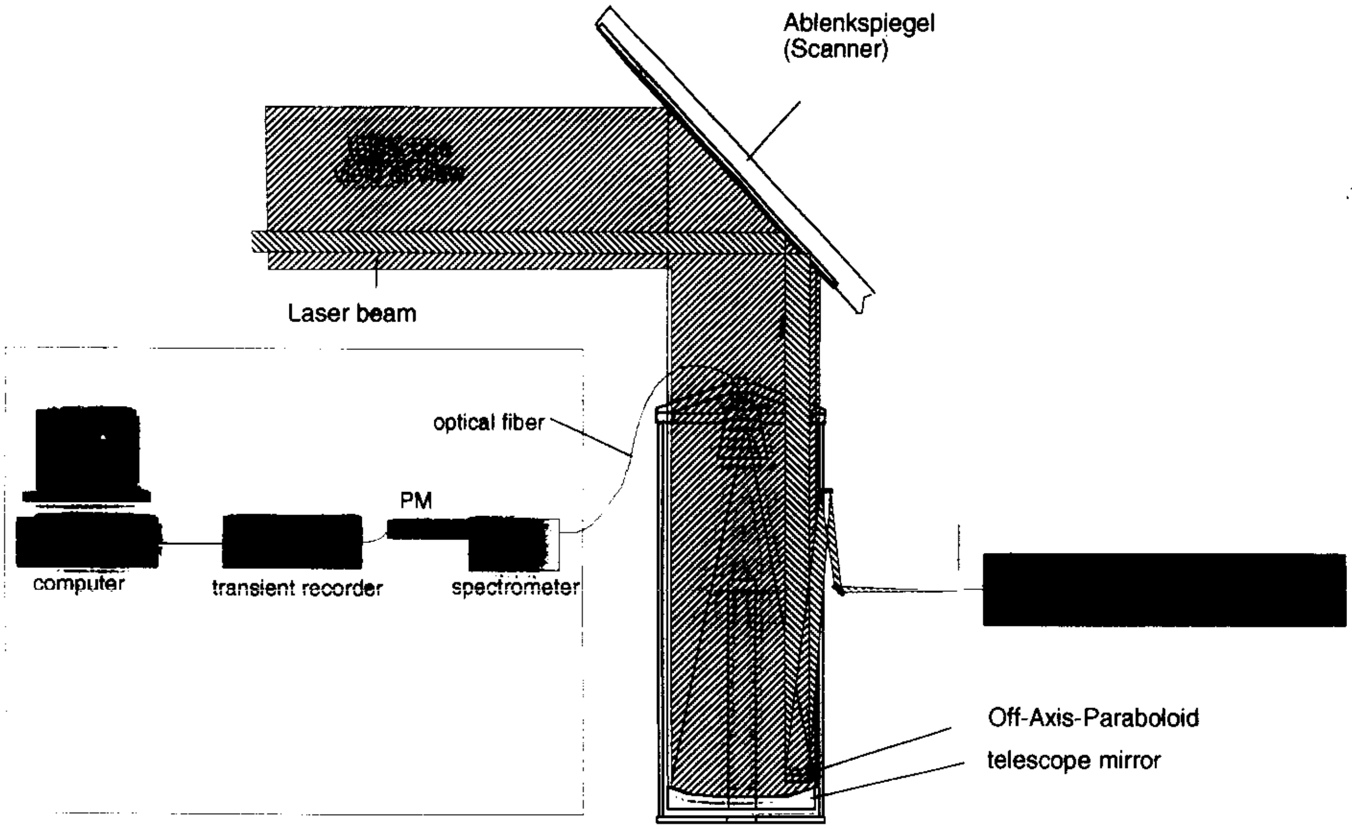

Hard Target DIAL Method

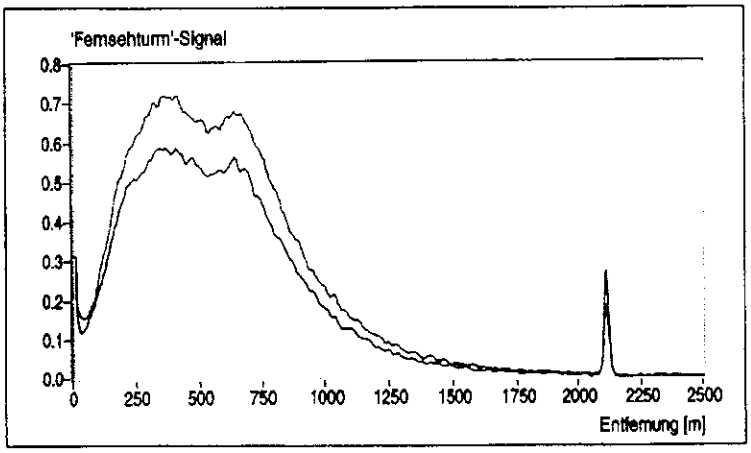

$$\ln \frac{P(\lambda_{off}, R_{FT})}{P(\lambda_{on}, R_{FT})} = 2\Delta R(\alpha(Toluol) + \alpha(O_3) + \alpha(O_2)$$

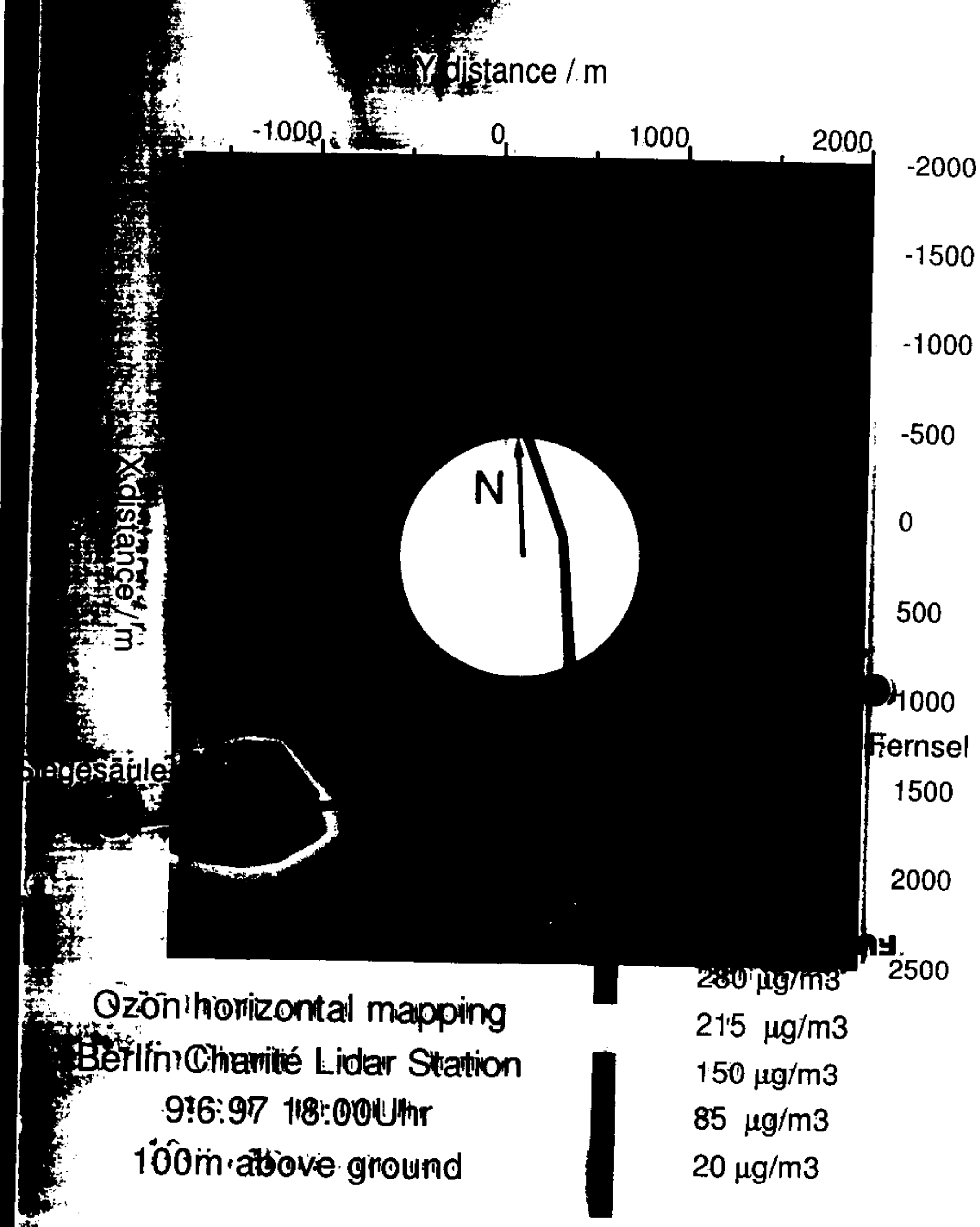
Y distance / m
-1000
0
1000
2000
-2000
-1500
-1000
-500
0
500
1000
1500
2000
2500
X distance / m
N
Fernsel
Siegesäule
280 µg/m3
215 µg/m3
150 µg/m3
85 µg/m3
20 µg/m3
Ozon horizontal mapping
Berlin Charité Lidar Station
9.6.97 18:00Uhr
100m above ground

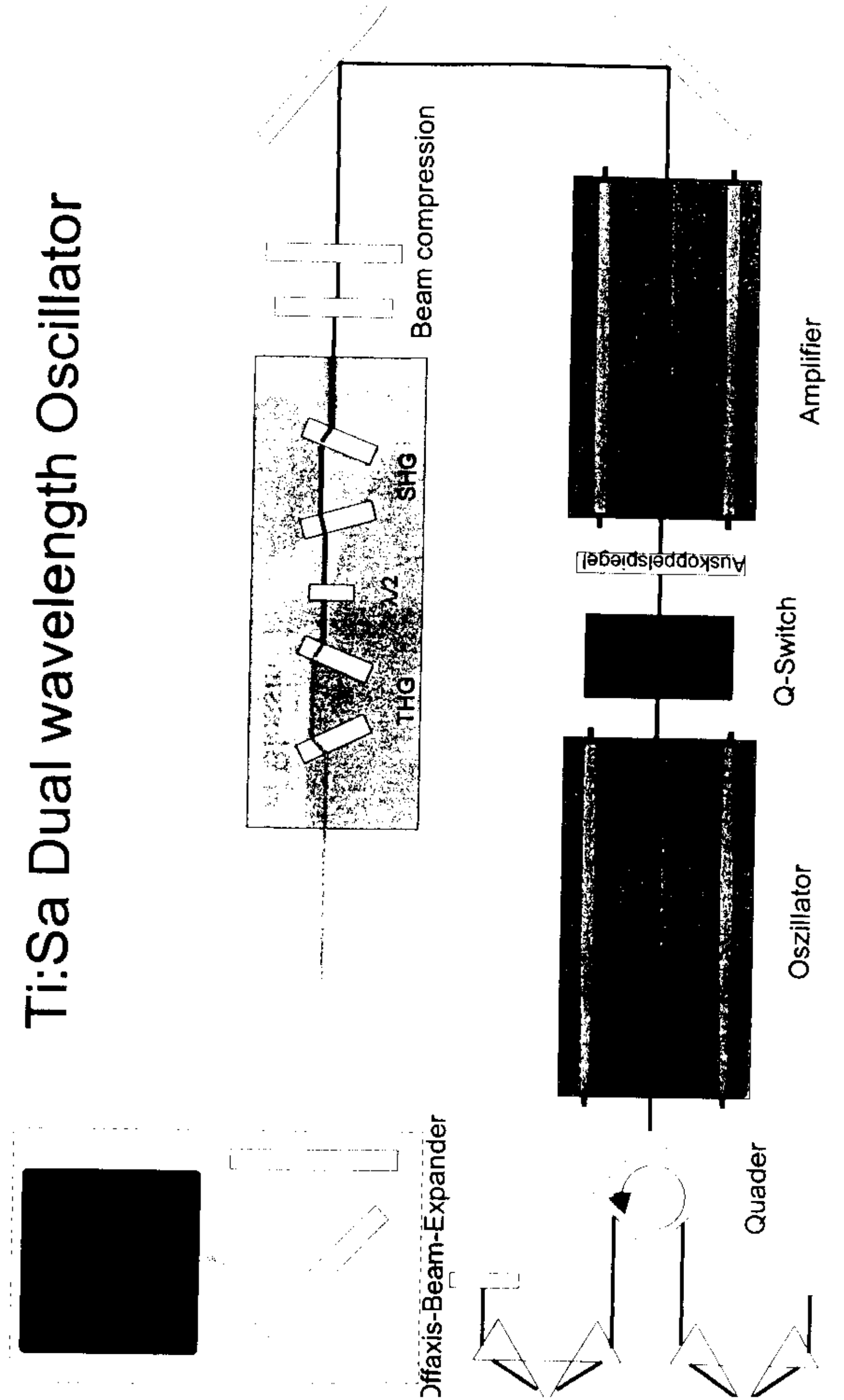
Ti:Sa Dual wavelength Oscillator
Beam compression
SHG
λ/2
THG
Amplifier
Auskoppelspiegel
Q-Switch
Oszillator
Quader
Offaxis-Beam-Expander

LIDAR Station 0(Ch), FU Berlin
vertical scans

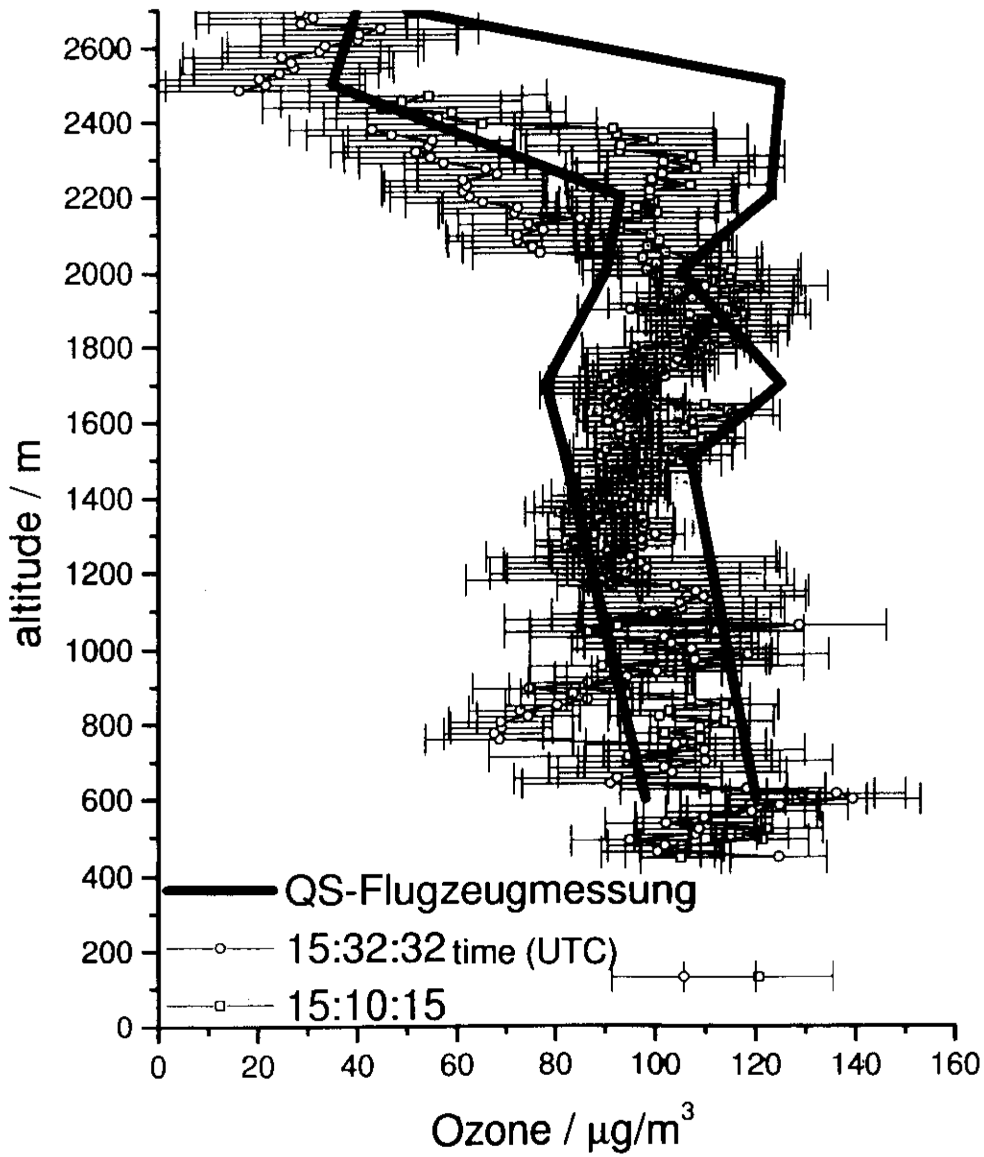

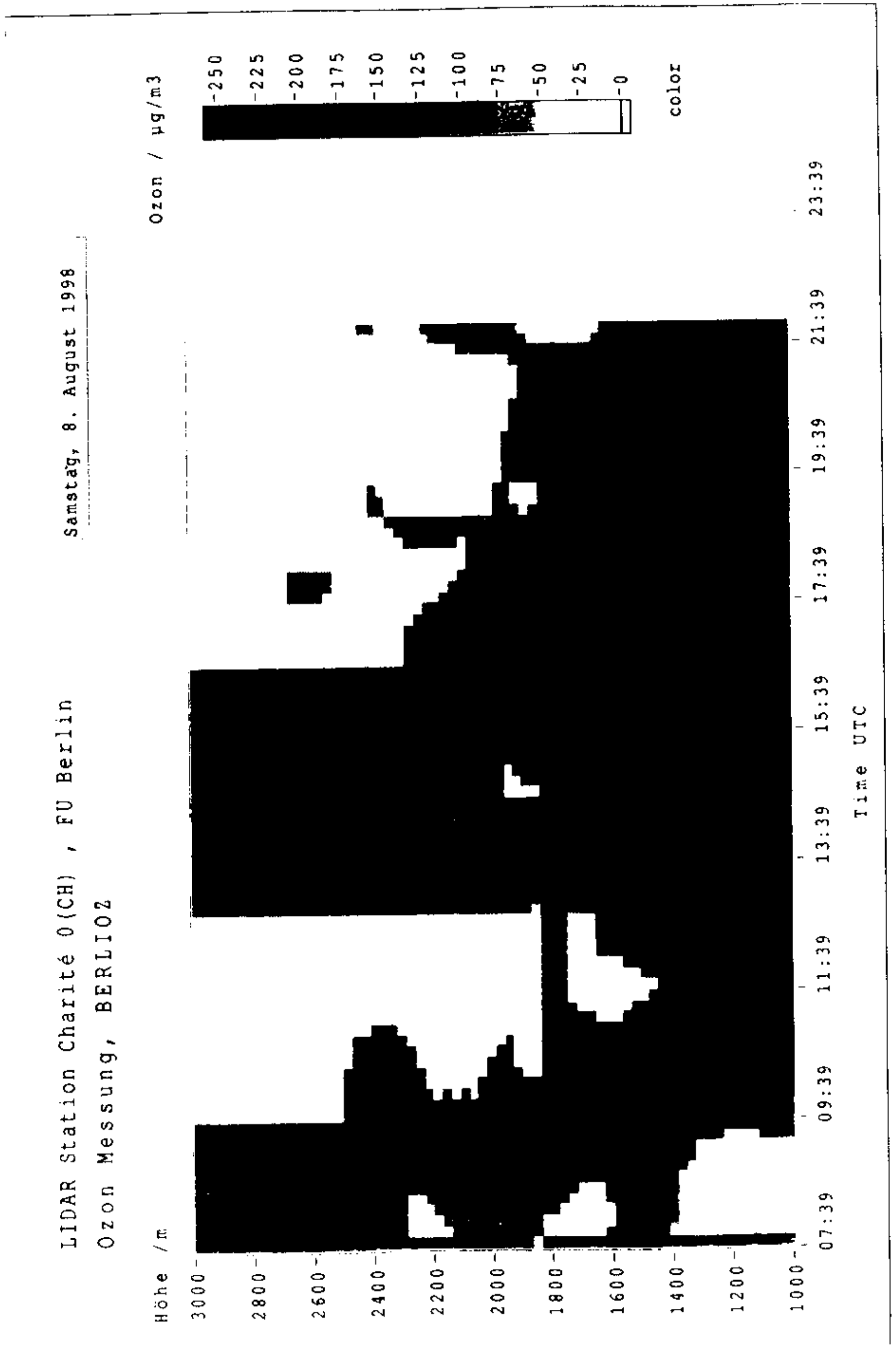

Atmospheric Remote Sensing

FTIR / DOAS

- Uses sun, moon or lamps as lightsource
- Many atmospheric trace gases can be measured simultanously
- Course or no range resolution

LIDAR (DIAL)

- Uses lasers as light source
- Only a few atmospheric species can be measured (O_3, NO, NO_2, CH_4, SO_2, water vapour, aerosols)
- No simultanous measurement
- High spatial and temporal resolution

GOAL:
Combine the advantages of Lidar and FTIR / DOAS

White Light Generation I: Self phase modulation

at high intensities: $n = n_0 + n_2 \cdot I$

$n_2 = 5.6 \cdot 10^{-13} \frac{cm^2}{W}$

$$\omega_m(t) = \omega_0 \left(1 - \frac{\ell}{c} \frac{dn(t)}{dt}\right)$$

$$\Delta\omega = \frac{\omega_0}{c} n_2 \frac{I \ell}{\Delta t}$$

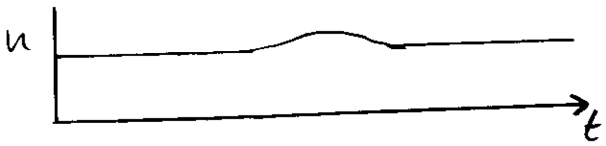

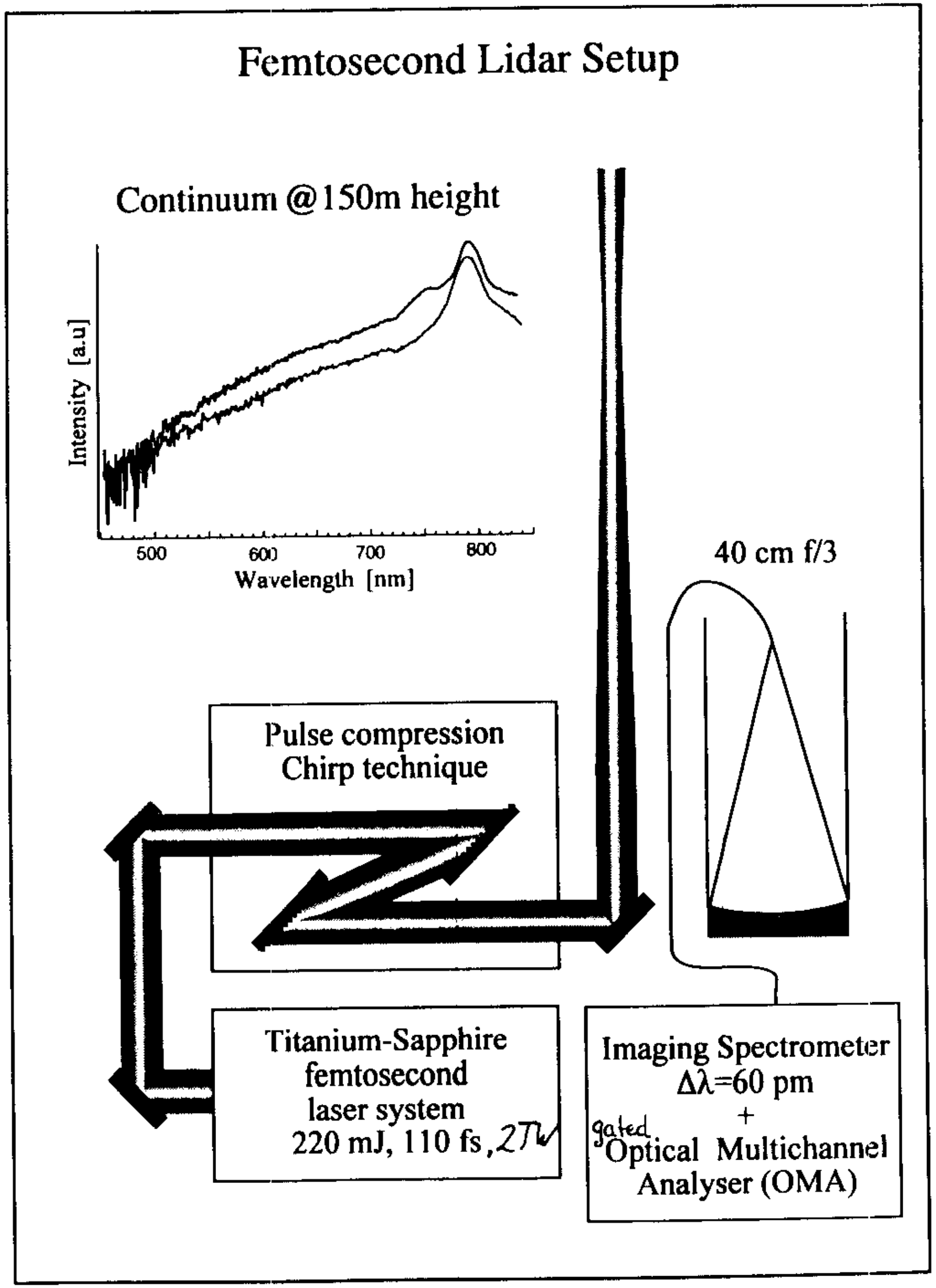

White light Lidar signals

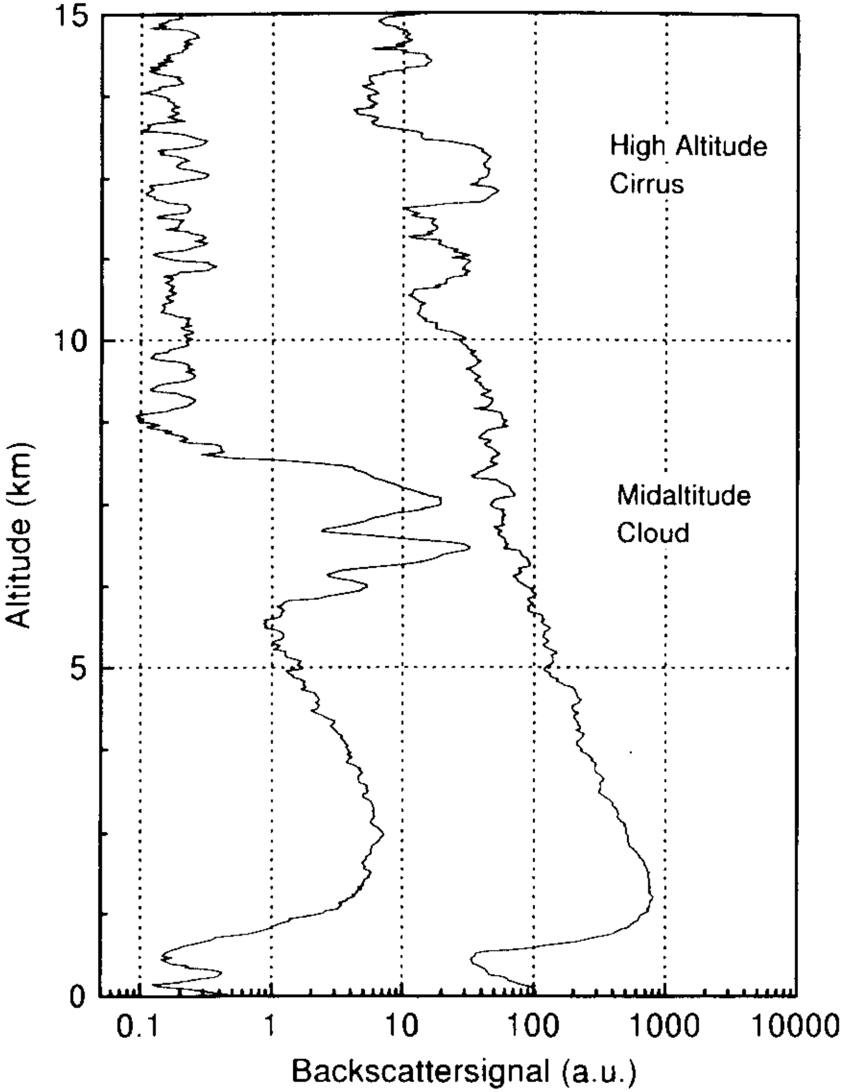

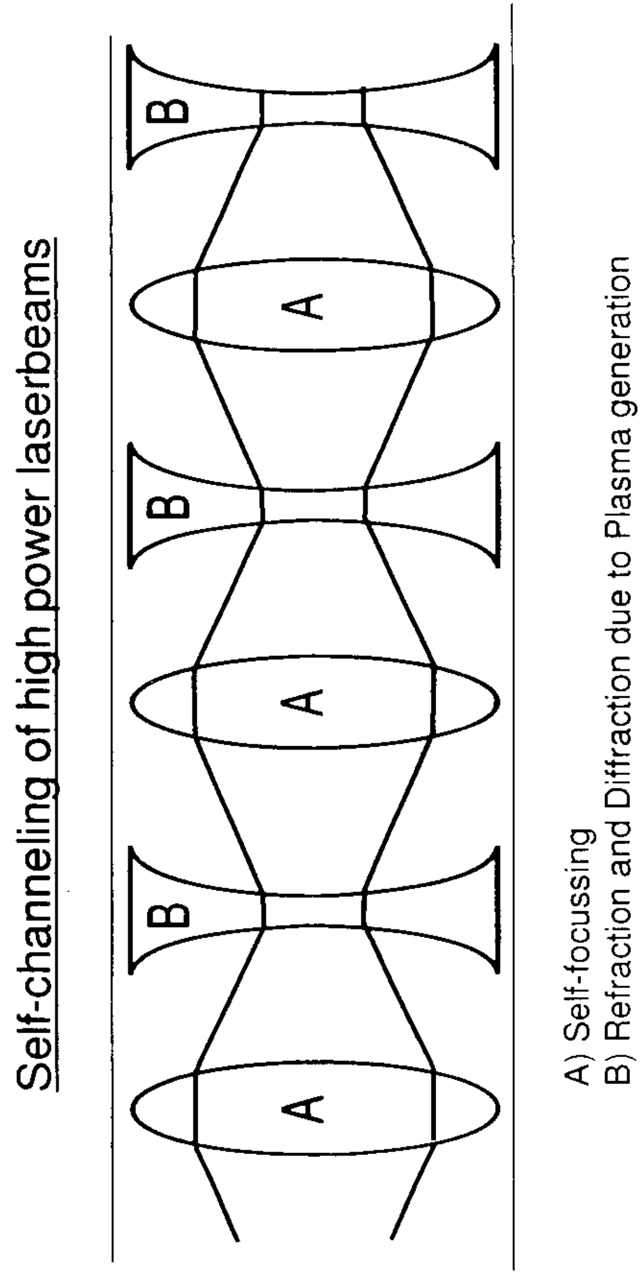

Water Vapor

Int.: 550-1100 m, 4 min, Mix. Ratio= 0.6 %

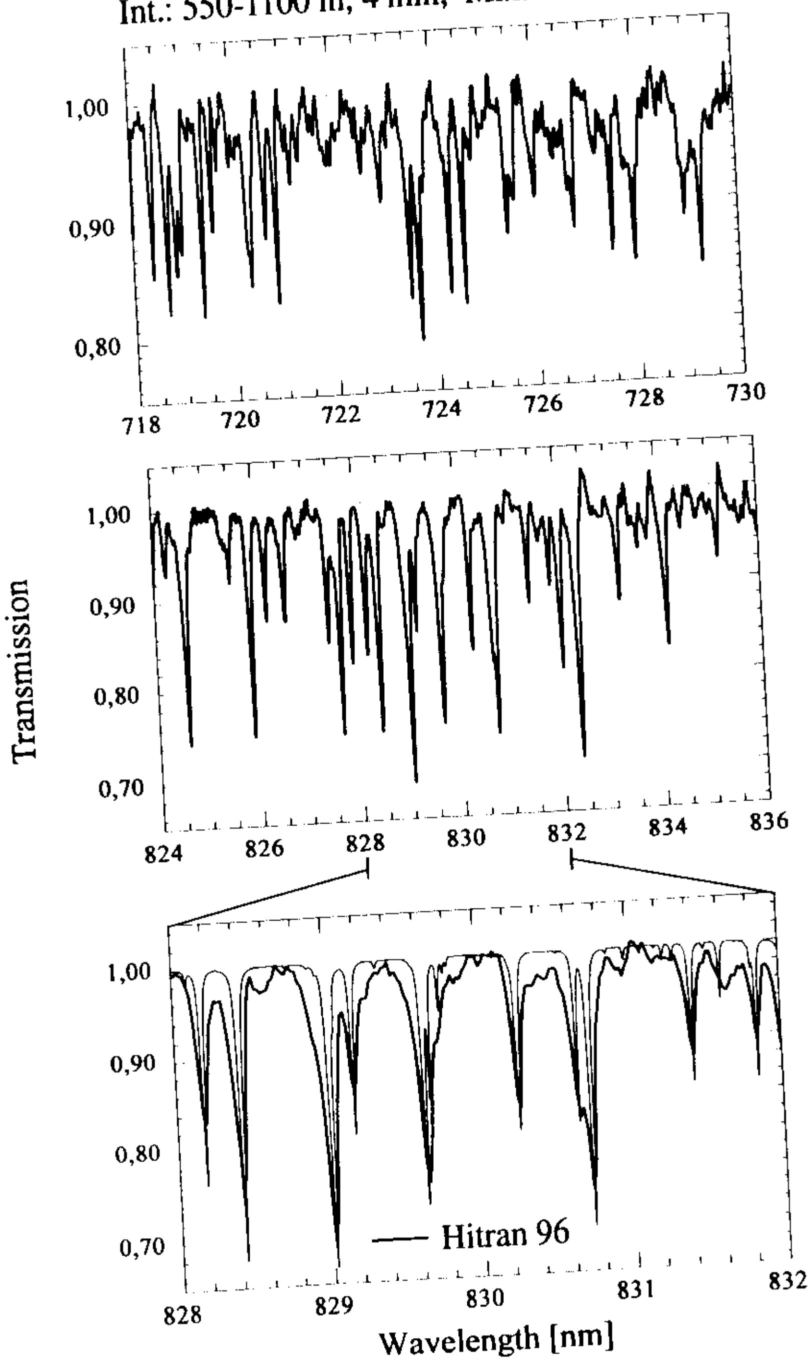

Oxygen O_2

Int.:600-800 m, 4 min